

# The third dredge-up and the carbon star luminosity functions in the Magellanic Clouds

Paola Marigo<sup>1,2</sup>, Léo Girardi<sup>1</sup>, Alessandro Bressan<sup>3</sup>

<sup>1</sup> Max-Planck-Institut für Astrophysik, Karl-Schwarzschild-Str. 1, D-85740 Garching bei München, Germany

<sup>2</sup> Department of Astronomy, University of Padova, Vicolo dell'Osservatorio 5, I-35122 Padova, Italy

<sup>3</sup> Astronomical Observatory, Vicolo dell'Osservatorio 5, I-35122, Padova, Italy

Received 20 October 1998 / Accepted 18 December 1998

**Abstract.** We investigate the formation of carbon stars as a function of the stellar mass and parent metallicity. Theoretical modelling is based on an improved scheme for treating the third dredge-up in synthetic calculations of thermally pulsing asymptotic giant branch (TP-AGB) stars. In this approach, the usual criterion (based on a constant minimum core mass for the occurrence of dredge-up,  $M_c^{\min}$ ) is replaced by one on the minimum temperature at the base of the convective envelope,  $T_b^{\text{dred}}$ , at the stage of the post-flash luminosity maximum. Envelope integrations then allow determination of  $M_c^{\min}$  as a function of stellar mass, metallicity, and pulse strength (see Wood 1981), thus inferring if and when dredge-up first occurs. Moreover, the final possible shut down of the process is predicted.

Extensive grids of TP-AGB models were computed by Marigo (1998ab) using this scheme. In this paper, we present and discuss the calibration of the two dredge-up parameters (i.e. efficiency  $\lambda$  and  $T_b^{\text{dred}}$ ) aimed at reproducing the carbon star luminosity function (CSLF) in the LMC, using TP-AGB models with original metallicity  $Z = 0.008$ . In addition to this, the effects of different input quantities on the theoretical CSLF are analysed. It turns out that the faint tail is almost insensitive to the history of star formation rate (SFR) in the parent galaxy, in contrast to the bright wing which may be more affected by the details of the recent history. Actually, we find that the faint end of the CSLF is essentially determined by the temperature parameter  $T_b^{\text{dred}}$ . Once the faint end is reproduced, the peak location is a stringent calibrator of the efficiency parameter  $\lambda$ . The best fit to the observed CSLF in the LMC is obtained with  $\lambda = 0.50$ ,  $\log T_b^{\text{dred}} = 6.4$ , and a constant SFR up to an age of about  $5 \times 10^8$  yr. This recent drop of the SFR is invoked to remove a slight excess of bright carbon stars otherwise predicted.

A good fit to the observed CSLF in the SMC is then easily derived from the  $Z = 0.004$  models, with a sim-

ple choice of parameters  $\lambda = 0.65$ ,  $\log T_b^{\text{dred}} = 6.4$ , and a constant SFR over the entire significant age interval. The result for  $\lambda$  is consistent with the theoretical expectation that the third dredge-up is more efficient at lower metallicities.

**Key words:** stars: evolution – stars: AGB and post-AGB – stars: mass-loss – stars: carbon – Magellanic Clouds

## 1. Introduction

During the TP-AGB phase, recurrent episodes of dredge-up can significantly affect the surface chemical composition of low- and intermediate-mass stars. These episodes are usually known as “the third dredge-up”. The basic mechanism of the mixing to the surface can be explained on the basis of the standard structure equations applied to stellar models in quasi-static evolution (Iben & Renzini 1983). During the peak of every flash in the helium shell, part of the nuclear energy is converted into thermal energy, and the remaining spent as mechanical work for the expansion of the overlying matter. Material at the hydrogen-helium ( $X - Y$ ) discontinuity and beyond is pushed outward so that the H-burning shell is temporarily extinguished. At the same time, the base of the convective envelope moves inward because of the progressive local raising of the radiative temperature gradient over the adiabatic one, triggered by the increase of the energy flux and the concomitant decline of the temperature consequent to the expansion.

Dredge-up occurs if the convective envelope can penetrate into the inter-shell region containing material that has just undergone helium burning during the flash. A certain amount of inter-shell matter is then brought up to the surface, and pollutes the envelope with newly synthesised nuclear products. The dredge-up material mainly consists of helium, carbon, oxygen and traces of heavy elements produced by s-process nucleosynthesis (see Lattanzio & Boothroyd 1997 for an extensive review of the topic).

The formation of single carbon (C-) stars is usually ascribed to the enrichment of  $^{12}\text{C}$  surface abundance produced by the third dredge-up. The topic is important for a series of reasons. First, C-stars are present in many Local Group galaxies, indicating the presence of relatively young stellar populations. The precise age and metallicity intervals relevant for the formation of C-stars, however, are far from being fully assessed from both theory and observations. Secondly, these stars are crucial for the interpretation of a series of chemical abundance data. For instance, it is believed that most SiC grains found in primitive meteorites are formed in extended carbon-rich envelopes of C-stars (Gallino et al. 1990). The emission features detected in the infrared spectra from extended circumstellar shells around AGB stars are significantly affected by the composition of the dust grains (Ivezic & Elitzur 1995). The variety of chemical abundance patterns in planetary nebulae probably reflects the different efficiency and duration of dredge-up episodes in the progenitor stars, as well as the possible burning of CNO isotopes at the base of their envelopes (the so-called hot-bottom burning or envelope burning; see Marigo et al. 1998 and references therein).

In recent years many investigations have been devoted to the analysis of the occurrence and related efficiency of the dredge-up, and to the nucleosynthesis driven by thermal pulses (Boothroyd & Sackmann 1988cd; Frost & Lattanzio 1996; Straniero et al. 1997; Lattanzio & Boothroyd 1997; Herwig et al. 1997; and references therein). The main challenge of the theory in this case is offered by the so-called *carbon star mystery*, first pointed out by Iben (1981). Observations of AGB stars in the Large and Small Magellanic Clouds (LMC and SMC) indicate that the luminosity range in which carbon stars are found extends down to rather faint magnitudes ( $M_{\text{bol}} \gtrsim -3$ ), thus suggesting the evolution from low-mass progenitors ( $M_1 \sim 1 - 3 M_{\odot}$ ). In contrast, complete AGB models easily explain the formation of carbon stars at much higher luminosities ( $M_{\text{bol}} < -5 - -6.5$ ), but fail to reproduce the faint part of the observed distribution, since dredge-up of carbon is hardly found to occur during the TP-AGB evolution of low-mass models.

Although some improvements have recently been attained (Frost & Lattanzio 1996; Straniero et al. 1997; Herwig et al. 1997) the present understanding of the dredge-up process is still unsatisfactory, mostly because of the uncertainties in the treatment of the mixing process and the definition of convective boundaries. In Sect. 2 we give an overview of the present state of art emerging from the available results of complete modelling of the third dredge-up, and discuss the role of analytical TP-AGB calculations in possibly giving useful theoretical indications.

In the present study, *the treatment of the third dredge-up in synthetic TP-AGB calculations has been significantly improved. A simple technique based on integrations of static envelope models is used in order to infer if and when convective dredge-up is likely to occur during the evo-*

*lution of a TP-AGB star.* In this way, we abandon the assumption of a constant parameter  $M_{\text{c}}^{\text{min}}$ , usually adopted in synthetic calculations (Groenewegen & de Jong 1993; Marigo et al. 1996a), and the dependence on the current stellar mass and metallicity is taken into account. The method is described in Sect. 3.

A primary target of theoretical models of the AGB phase is the interpretation and reproduction of the observed CSLFs in the Magellanic Clouds (Sect. 4). This is because a sole observable holds a number of profound implications for different physical processes occurring in AGB stars (e.g. nucleosynthesis, mixing and surface chemical enrichment, mass-loss), and sets at the same time severe constraints both on theoretical prediction of stellar parameters (e.g. evolutionary rates, luminosities, lifetimes, initial mass of carbon stars' progenitors), and possibly on properties of the related stellar populations to which carbon stars belong (e.g. the history of star formation). Section 5 illustrates the derivation of theoretical CSLFs.

In this study the formation of carbon stars is investigated with the aid of the parameterized treatment of the third dredge-up. In Sect. 6, the dredge-up parameters (efficiency  $\lambda$ , and base temperature  $T_{\text{b}}^{\text{dred}}$  of the envelope at the post-flash luminosity peak) are first determined by demanding that the theoretical CSLF, calculated for initial metallicity  $Z = 0.008$ , suitably fits the distribution observed in the LMC. This calibration is important not only for deriving theoretical indications on the dredge-up process itself, but also because it gives more reliability to the analysis on the surface chemical composition of AGB stars and related applications (e.g. estimation of chemical yields, and chemical abundances in planetary nebulae). The sensitivity of the results to the underlying history of star formation and the initial mass function (IMF) is also explored.

The same procedure is then applied to find the proper pair of parameters to reproduce the CSLF in the SMC (Sect. 7). In this case evolutionary calculations for initial metallicity  $Z = 0.004$  are used. The differences between the LMC and SMC distributions are discussed. Section 8 summarises our main conclusions.

## 2. The role of synthetic calculations

The usual analytical treatment of the third dredge-up requires the knowledge of three basic input quantities:

- the minimum core mass for dredge-up to occur  $M_{\text{c}}^{\text{min}}$ ;
- the dredge-up efficiency  $\lambda$ ;
- the chemical composition of the convective inter-shell.

A TP-AGB star can experience the third dredge-up when its core mass has grown over a critical value  $M_{\text{c}}^{\text{min}}$ , as indicated by theoretical analyses of thermal pulses (e.g. Wood 1981; Iben & Renzini 1983; Boothroyd & Sackmann 1988cd; Lattanzio 1989). Estimates of  $M_{\text{c}}^{\text{min}}$  based

**Table 1.** The third dredge-up in low-mass stars according to full TP-AGB calculations. For given stellar mass  $M_i$ , envelope abundances (in mass fraction) of hydrogen  $X$  and helium  $Y$ , and adopted mixing-length parameter  $\alpha$ , the core mass  $M_c^{\text{min}}$  at the onset of dredge-up (if found) is given. The value of the bolometric magnitude,  $M_{\text{bol}}(M \rightarrow C)$ , corresponds to the pre-flash maximum quiescent luminosity marking the transition to carbon star. The estimates inside parenthesis refer to the faintest luminosity during the post-flash luminosity dip.

$M_i (M_\odot)$	$Z$	$Y$	$\alpha$	$M_c^{\text{min}} (M_\odot)$	$M_{\text{bol}}(M \rightarrow C)$	Source
3.0	0.020	0.28	1.0	no dredge-up	—	Wood (1981)
3.0	0.020	0.28	1.7	0.58	–not given–	Herwig et al. (1997)
3.0	0.020	0.28	2.2	0.611	–5.66	Straniero et al. (1997)
2.0	0.020	0.30	1.5	no dredge-up	—	Gingold (1975)
1.7	0.001	0.28	1.0	no dredge-up	—	Wood (1981)
1.7	0.001	0.26	1.5	0.665	–5.11 (–4.68)	Boothroyd & Sackmann (1988d)
1.5	0.001	0.28	1.0	no dredge-up	—	Wood (1981)
1.5	0.001	0.20	1.5	0.605	— (–4.0)	Lattanzio (1989)
1.5	0.003	0.30	1.5	0.69	–not given–	Lattanzio (1987)
1.5	0.003	0.20	1.5	0.62	–5.20	Lattanzio (1986)
1.5	0.004	0.25	1.6	no dredge-up	—	Vassiliadis & Wood (1993)
1.5	0.006	0.30	1.5	0.70	–not given–	Lattanzio (1986)
1.5	0.020	0.30	1.0	no dredge-up	—	Lattanzio (1987)
1.5	0.020	0.28	2.2	0.63	–5.65	Straniero et al. (1997)
1.5	0.020	0.20	1.5	0.635	— (< –4.8)	Lattanzio (1989)
1.0	0.021	0.24	1.5	no dredge-up	—	Schönberner (1979)
1.0	0.001	0.20	1.5	0.630	— (–4.3)	Lattanzio (1989)
0.8	0.001	0.26	3.0	0.566	–4.35 (–3.59)	Boothroyd & Sackmann (1988d)
0.7	0.001	0.25	1.5	0.612	–not given–	Iben & Renzini (1982)
0.6	0.001	0.30	1.5	no dredge-up	—	Gingold (1974)

on complete evolutionary calculations are still a matter of debate, since this quantity depends on the delicate interplay between model prescriptions (e.g. opacities, nuclear reaction rates, convection theory, mass-loss, time and mass resolution) and intrinsic properties of the star (e.g. chemical composition, envelope mass, strength of the thermal pulses). In Table 1 we report some values of  $M_c^{\text{min}}$  taken from different authors. It turns out that the results vary remarkably, even among models with the same total mass and metallicity. The third dredge-up is often not found in low-mass models, and if it is, the corresponding metallicities are quite low and the transition luminosities [see the  $M_{\text{bol}}(M \rightarrow C)$  entry] are in most cases still brighter than the faint wing of the CSLFs in the Magellanic Clouds. Nevertheless, a certain trend can be extracted from the comparison of the results, i.e. the onset of the third dredge-up is favoured at higher stellar mass  $M$ , lower metallicity  $Z$ , and greater efficiency of envelope convection (obtained e.g. by increasing the mixing-length parameter  $\alpha$ ).

The parameter  $\lambda$  expresses the dredge-up efficiency. It is defined as the fraction of the core mass increment over the preceding inter-pulse period,  $\Delta M_c$ , which is dredged-up to the surface by the downward penetration of the convective envelope:

$$\lambda = \frac{\Delta M_{\text{dredge}}}{\Delta M_c} \quad (1)$$

where  $\Delta M_{\text{dredge}}$  is the mass of the dredged-up material.

The question of the true value of  $\lambda$  is also troublesome. The effective penetration of the envelope is crucially affected by the treatment of the instability of matter against convection, still poorly understood. In the standard approach, the boundary of a convective region is defined by the Schwarzschild criterion, i.e. where the inward gravity force is balanced by the buoyancy force. However, at this point the velocity of the convective eddies is not null, so that they can effectively penetrate into formally stable regions. This phenomenon is usually known as convective overshoot. Over the years, several attempts have been made in order to include this effect into evolutionary calculations (see Chiosi et al. 1992 and references therein). However, at present it appears that there is no real agreement among different authors on the criterion to define the maximum inward penetration of the envelope at thermal pulses during the AGB. Moreover, the results seem to depend quite sensitively on technical and numerical details (see Frost & Lattanzio 1996 for a discussion of this aspect).

The heterogeneous situation is well represented by the two following examples. On the one side, Straniero et al. (1997) obtain rather efficient dredge-up just using the Schwarzschild criterion and without invoking any extra-mixing, but drastically increasing both time and mass resolution during calculations. On the other hand, Herwig et al. (1997) find deep extra-mixing during dredge-up on the basis of a parameterized description of the overshoot

region, built up to mimic the indications from hydrodynamical simulations (Freytag et al. 1996) of convection in stars of a different kind (i.e. main sequence stars and white dwarfs).

As far as the efficiency of the third dredge-up is concerned, it is not easy to summarise the results from different authors. However, suffice it to recall that recurrent estimates, derived from TP-AGB calculations of low-mass stars, give at most  $\lambda \sim 0.3 - 0.4$  and often even smaller (Iben & Renzini 1984; Lattanzio 1986, 1987, 1989; Boothroyd & Sackmann 1988d; Straniero et al. 1997).

In conclusion, the present state of art is the following. On the one hand, most authors still do not find significant dredge-up in their calculations (Vassiliadis & Wood 1993; Wagenhuber 1996; see also Table 1), or assume the efficiency  $\lambda$  as an input quantity (Forestini & Charbonnel 1997). On the other hand, the difficulty of a too poor dredge-up in low-mass stars seems to be overcome to some extent (Boothroyd & Sackmann 1988d; Frost & Lattanzio 1996; Straniero et al. 1997; Herwig et al. 1997), but extensive calculations over a wide range of stellar masses and metallicities are required to test the results by means of a meaningful comparison with observations. Moreover, results are quite different even for similar initial conditions (e.g.  $M$  and  $Z$ ).

A powerful investigation tool complementary to full calculations is offered by synthetic TP-AGB models, which have been notably improved and up-graded in recent years (Groenewegen & de Jong 1993; Marigo et al. 1996a, 1998; Marigo 1998ab). As far as the third dredge-up is concerned, synthetic TP-AGB calculations clearly suggest that a higher efficiency is required (e.g.  $\lambda \sim 0.65 - 0.75$ ) in order to reproduce observational constraints (e.g. the CSLF in the LMC), a goal still missed by complete modelling of the TP-AGB phase.

The use of the parameters  $M_c^{\min}$  and  $\lambda$  plays a relevant role in analytical models of the TP-AGB phase. They both significantly affect the predicted luminosity functions of carbon stars, in particular the position of the peak and the low-luminosity tail of the distribution. Lowering  $M_c^{\min}$  favours the formation of carbon stars of lower masses and at the same time results in a longer carbon star phase; increasing  $\lambda$  corresponds to a higher fraction of low mass stars which become carbon stars at fainter luminosities. In Marigo et al. (1996a) it was simply assumed that both  $M_c^{\min}$  and  $\lambda$  were constant, thus neglecting their likely dependence on the stellar metallicity, total mass, core mass, and mixing length parameter. Though being a rough approximation, such a choice was meant to provide useful theoretical indications. The calibration of the dredge-up parameters was based on the goal of reproducing the observed CSLFs in the LMC. It resulted that the suitable values were  $M_c^{\min} = 0.58 M_\odot$  and  $\lambda = 0.65$ . These values are very close to those derived by Groenewegen & de Jong (1993). Basing on these results, Forestini & Charbonnel (1997) fixed  $\lambda = 0.6$  in their full calculations, in

order to estimate the chemical yields from intermediate-mass stars.

### 3. The minimum core mass for dredge-up

In this section we illustrate the adopted scheme which replaces the assumption of a constant  $M_c^{\min}$ . To start with, it is necessary to consider some indications about the dredge-up provided by detailed calculations of thermal pulses. They show that the maximum inward penetration of the envelope convection, over the pulse cycle, occurs when the surface luminosity attains its characteristic post-flash peak,  $L_P$  (Wood 1981; Wood & Zarro 1981; Boothroyd & Sackmann 1988d). Dredge-up takes place if the envelope convection zone is able to penetrate into the carbon enriched region previously occupied by the inter-shell convection zone during the flash.

In Sects. 3.1 and 3.2 below we recall and discuss the features which are relevant to our analysis on the occurrence of the dredge-up, namely the behaviour of the peak luminosity  $L_P$ , and the temperature at the base of the convective envelope during the dredge-up events. In Sect. 3.3 the method to infer  $M_c^{\min}$  for each AGB model is described, and the results for several values of the stellar mass and metallicity are presented. Section 3.4 details the adopted inter-shell composition.

#### 3.1. The $M_c - L_P$ relation

Wood & Zarro (1981) and Wood (1981) pointed out that at the surface luminosity maximum the outward-flowing luminosity,  $L_r$ , is almost constant (to a fraction of a percent) throughout the envelope, from the top of the remnant inter-shell convection zone to the surface. This is because the thermal timescale in the envelope (i.e. for absorption/release of internal-gravitational energy during the hydrostatic re-adjustment following the flash) is much shorter (i.e. few years) than the evolutionary timescale for the envelope structure to be changed (i.e. decades to centuries). The constancy of  $L_r$  may no longer be true when significant energy absorption can occur in the envelope, e.g. in stars with quite massive envelopes ( $M_{\text{env}} > 2.5 M_\odot$ ), or large core masses ( $M_c > 0.9 M_\odot$ ) (Wood & Zarro 1981).

The fact that at the post-flash luminosity maximum the envelope is close to hydrostatic and thermal equilibrium (Wood 1981), together with the existence of a radiative buffer over the burning shell, constitute the necessary physical conditions which secure the validity of the so-called zero-order-radiative-approximation (Schwarzschild 1958; Eggleton 1967; Paczyński 1970; Wood & Zarro 1981). In brief, theory shows that  $L_P$  is essentially controlled by the core mass of the star independently of the outer envelope mass, in analogy with the existence of the  $M_c - L$  relation during the quiescent inter-pulse periods for low-mass AGB stars. For more details on the basic con-

ditions that underlie the theory of a core mass-luminosity relationship, the reader is referred to Refsdal & Weigert (1970), Kippenhahn (1981) and Tuchman et al. (1983); see also Boothroyd & Sackmann (1988b) and references therein.

In this study we adopt the  $M_c - L_P$  relation presented by Wagenhuber & Groenewegen (1998), derived from extensive calculations of complete AGB models (Wagenhuber 1996). It expresses the post-flash luminosity maximum as the sum of two terms, i.e.  $L_P = L_{(P,\text{full})} + \Delta L_{(P,\text{first})}$ , where

$$L_{(P,\text{full})} = [93000 + 2758 \log(Z/0.02)] \times \{M_c - [0.503 + 0.82(Z - 0.02)]\} \quad (2)$$

and

$$\Delta L_{(P,\text{first})} = -10^{[1.77 + 2.76M_{c,0} - (34.0 + 32.4M_{c,0})\Delta M_c]} \quad (3)$$

The former term [Eq. (2)] gives the post-flash luminosity maximum (in  $L_\odot$ ) for full-amplitude thermal pulses as a function of  $M_c$  (in  $M_\odot$ ), with a dependence on the metallicity  $Z$  (in mass fraction). The latter term [Eq. (3)] represents a negative correction which has to be added to  $L_{(P,\text{full})}$  in order to reproduce the fainter maximum in the light-curve (at given  $M_c$ ) for the first pulses, expressed as a function of the core mass at the first He-shell flash,  $M_{c,0}$ , and the current core mass increment,  $\Delta M_c = M_c - M_{c,0}$ .

### 3.2. A characteristic temperature for dredge-up

Following Wood (1981), at the post-flash luminosity peak the envelope convection reaches its maximum inward penetration (in mass fraction) and base temperature,  $T_b^{\text{max}}$ . At the same time, the nuclearily processed material involved in the He-shell flash is pushed out and cooled down to its minimum temperature over the flash-cycle,  $T_N^{\text{min}}$ .

To this respect, a very interesting and useful indication is given by Wood (1981), who reported that at the stage of post-flash luminosity maximum, the temperature  $T_N^{\text{min}}$  always approaches a limiting constant value ( $\log T_N^{\text{min}} = 6.7 \pm 0.1$ ), for all core masses studied ( $0.57 M_\odot \leq M_c \leq 0.88 M_\odot$ ), regardless of the metallicity ( $Z = 0.001$ ,  $Z = 0.01$ , and  $Z = 0.02$ ).

A similar remark can be found in the work by Boothroyd & Sackmann (1988d) about the production of low-mass carbon stars. In the final discussion the authors stated that “it is probably no coincidence” that in all cases considered (i.e. full AGB calculations for stars with total mass and metallicity [ $M_i = 0.8 M_\odot, Z = 0.001$ ], [ $M_i = 1.2 M_\odot, Z = 0.0022$ ], [ $M_i = 1.7 M_\odot, Z = 0.001$ ], and [ $M_i = 2.0 M_\odot, Z = 0.001$ ]) the first episode of convective dredge-up is characterised by a temperature at the base of the convective envelope of approximately the same value,  $\log T_b^{\text{max}} \sim 6.5$ . In other words,  $T_b^{\text{max}} \sim T_N^{\text{min}}$  at the first occurrence of the third dredge-up.

In conclusion, detailed analyses of thermal pulses suggest that the third dredge-up takes place when the base

temperature attains or exceeds some critical value. Hereinafter, we will refer to it as  $T_b^{\text{dred}}$ . Therefore, we adopt the following criterion:

- if  $T_b^{\text{max}} < T_b^{\text{dred}} \Rightarrow$  no dredge-up can occur
- if  $T_b^{\text{max}} \geq T_b^{\text{dred}} \Rightarrow$  dredge-up occurs

On the basis of the above considerations, it is natural to assume that the fulfilment of the condition

$$T_b^{\text{max}} = T_b^{\text{dred}} \quad (4)$$

for the first time during the evolution marks the onset of dredge-up.

### 3.3. $M_c^{\text{min}}$ from envelope integrations

Thanks to the fact that at the time of the maximum penetration of the external convection the envelope is in hydrostatic and thermal equilibrium (Sect. 3.1), and that  $T_b^{\text{max}} \geq T_b^{\text{dred}}$  when dredge-up occurs (Sect. 3.2), it follows that the question of the minimum core mass for dredge-up can be analysed with the aid of a stationary envelope model.

Envelope integrations are performed on the basis of the following scheme. According to the analytical demonstration of Tuchman et al. (1983) it turns out that in the zero-order-radiative-approximation (see also Schwarzschild 1958; Eggleton 1967; Paczyński 1970) the product of the temperature  $T_c$  and radius  $R_c$  just above the burning shell, depends on the surface luminosity, core mass  $M_c$ , and chemical composition of the radiative transition region:

$$\left(\frac{T_c}{10^7}\right) R_c = \frac{2.291}{(5X + 3 - Z)} \left[ M_c - 0.156(1 + X) \frac{L}{10^4} \right] \quad (5)$$

where  $T_c$  is given in K,  $L_c$ ,  $M_c$  and  $R_c$  are expressed in solar units,  $X$  and  $Z$  are the abundances (in mass fraction) of hydrogen and metals, respectively. It is worth specifying that the term  $(5X + 3 - Z)$  comes from the definition of the mean molecular weight under the assumption of a fully ionised gas,  $\mu = 4/(5X + 3 - Z)$ , and the term  $(1 + X)$  derives from the expression of the opacity given by the Thomson scattering of electrons,  $\kappa = 0.2(1 + X)$ .

Equation (5) offers the boundary condition adopted here to determine the envelope structure of an AGB star at the luminosity-peak, i.e. the radius  $R_c$  of the spherical layer below which the mass  $M_c$  is contained, must coincide with:

$$R_c = \left(\frac{10^7}{T_c}\right) \frac{2.291}{(3 - Z_{\text{sh}})} \left[ M_c - 0.156 \frac{L_P}{10^4} \right] \quad (6)$$

Equation (6) is derived from Eq. (5) with  $L = L_P$  as given by Eqs. (2) and (3), setting  $X = 0$  since in this particular case we deal with material that has already undergone complete H-burning. The metallicity  $Z_{\text{sh}}$  is that of the inter-shell, i.e.  $Z_{\text{sh}} = X(^{12}\text{C}) + X(^{16}\text{O}) + Z \sim 0.24$  according to the prescription given in Sect. 3.4. Moreover, we

assume a constant value of the temperature,  $T_c = 10^8$  K, which gives a reasonable order of magnitude of the minimum temperature for the ignition of helium. The sensitivity of the results to  $T_c$  is discussed in Sect. 3.3.1 below.

Then, for given stellar mass, core mass, surface chemical composition, and peak-luminosity  $L_P$ , envelope integrations are performed until we find the value of the effective temperature,  $T_{\text{eff}}$ , such that  $M(R_c) = M_c$ . At this point, the structure of the envelope is entirely and uniquely determined.

### 3.3.1. Consistency checks

The consistency of our prescriptions must be checked. First, the assumption of a constant  $T_c = 10^8$  K seems to be arbitrary. However, we checked that varying this temperature by as much as 1 dex – far more than allowed by reasonable changes in the He-burning reaction rates – produces quite negligible changes on the results of envelope integrations (e.g. the values of  $T_b^{\text{max}}$ ,  $T_{\text{eff}}$ ,  $M_c^{\text{min}}$ ; see Table 1). Such invariance is just expected, given the physical decoupling between the core and the envelope as the  $M_c - L_P$  relation holds.

Actually, from the above discussion on the parameter  $T_c$ , it follows that the envelope structure is also quite insensitive to the corresponding value of  $R_c$ . Nevertheless, it is a useful exercise estimating  $R_c$  in an independent way and comparing it with the predictions from Eq. (5).

Following the formalism of Tuchman et al. (1983), the core of an AGB star behaves essentially as a *warm dwarf* of radius:

$$R_{\text{warm}}(M_c, T) = k(M_c, T) R_{\text{cold}}(M_c) \quad (7)$$

The term *warm dwarf* here indicates an isothermal electron-degenerate stellar core with non-zero temperature. The radius,  $R_{\text{cold}}$ , of a *cold dwarf* (defined at zero temperature) is a function of its mass (and chemical composition) only, whereas the radius of a *warm dwarf* is larger and depends on the temperature too. The ratio  $R_{\text{warm}}/R_{\text{cold}}$  is expressed via the factor  $k(M_c, T)$  in Eq. (7), which increases with  $T$  and decreases with  $M_c$ . However, Tuchman et al. (1983) pointed out that  $k$  typically ranges from 1 to 3 for relevant burning shells and  $M_c \gtrsim 0.6 M_\odot$ .

The radius  $R_{\text{cold}}$  is calculated adopting the linear fit to the Chandrasekhar (1939) results, as given by Tuchman et al. (1983):

$$R_{\text{cold}} = 0.019(1 - 0.58M_c) \quad (8)$$

where the quantities are expressed in solar units.

Figure 1 shows  $R_c$  as function of  $M_c$ , calculated according to Eq. (6) with  $T_c = 10^8$  K for three values of the envelope metallicity,  $Z = 0.004$ ,  $Z = 0.008$ , and  $Z = 0.019$ . The radius  $R_{\text{warm}}$  as derived from Eq. (7) for four different values of  $k$  is also plotted. For such a choice of the parameter  $T_c$ , the radius  $R_c$  turns out to be roughly  $3 \times R_{\text{cold}}$ , in

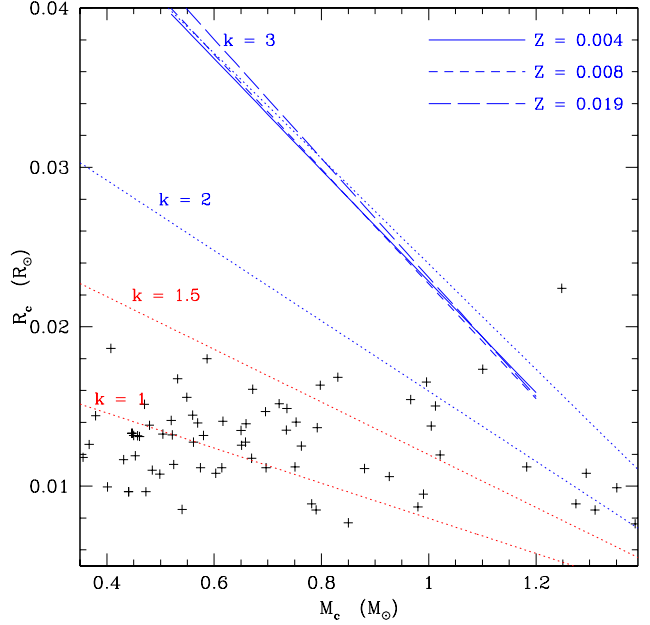


**Fig. 1.** The adopted core radius – core mass relationship for three different values of the metallicity  $Z$ , derived from Eq. (6) with  $T_c = 10^8$  K. The radius  $R_{\text{warm}}$  calculated with Eq. (7) is shown for few values of  $k$ , in the range 1 – 3. The data corresponds to the empirical white dwarf mass-radius relation (Koester 1987; Schmidt 1995; Koester & Reimers 1996).

agreement with the expected behaviour of *warm dwarfs*, and it is mostly comprised within  $0.04 R_\odot$  and  $0.02 R_\odot$  for the relevant range of  $M_c$  in AGB stars. Finally, for the sake of comparison, the empirical data on the white dwarf mass-radius relation (Koester 1987; Schmidt 1995; Koester & Reimers 1996) is also shown. It is worth noticing that the observed points are mostly consistent with  $1.5 \lesssim k \lesssim 1$ . This confirms the theoretical expectation that white dwarfs approach the zero-temperature configuration of complete degeneracy.

### 3.3.2. The choice of $T_b^{\text{dred}}$

On the basis of the scheme just outlined, *the minimum core mass for dredge-up of a model star of given total mass and surface chemical composition is found (if it exists) when the condition of Eq. (4) is satisfied for a unique pair of  $(L_P, T_{\text{eff}})$  values.*

The method represents a considerable improvement since we can obtain useful indications about the dependence of  $M_c^{\text{min}}$  on the envelope mass, metallicity, and peak strength, an important aspect so far ignored in previous synthetic AGB calculations (see Groenewegen & de Jong 1993; Marigo et al. 1996a).

There is one more prescription to be discussed, i.e. the adopted value of the characteristic temperature for

**Table 2.** Results from envelope integrations for a ( $2.0 M_{\odot}, Z = 0.004$ ) model at the stage of the post-flash luminosity maximum for given ( $L_P, M_c$ ) pair. Relevant quantities are shown as a function of different choices of the input parameter  $T_c$  [see Eq. (5)]. The minimum core mass for dredge-up,  $M_c^{\min}$ , is derived assuming  $\log T_b^{\text{dred}} = 6.4$ .

$M_c/M_{\odot}$	$\log(L_P/L_{\odot})$	$\log(T_c/10^7 \text{ K})$	$\log(R_c/\text{cm})$	$\log(T_{\text{eff}}/\text{K})$	$\log(T_b^{\text{max}}/\text{K})$	$M_c^{\min}/M_{\odot}$
0.5400	3.6598	0.8	9.6328	3.580637	6.48485	0.52551
		1.0	9.4328	3.580642	6.48461	0.52556
		1.2	9.2328	3.580648	6.48440	0.52563
		1.4	9.0328	3.580654	6.48408	0.52569
		1.6	8.8328	3.580660	6.48379	0.52576
		1.8	8.6328	3.580667	6.48346	0.52584

convective dredge-up,  $T_b^{\text{dred}}$ . As already mentioned, indications come from detailed analyses of thermal pulses, such as  $\log T_b^{\text{dred}} \sim 6.7$  in the work by Wood (1981), and  $\log T_b^{\text{dred}} \sim 6.5$  found by Boothroyd & Sackmann (1988d).

Wood (1981) first performed a similar kind of analysis adopted here to infer  $M_c^{\min}$  from envelope integrations. The author aimed at investigating the theoretical incapability of reproducing the observed carbon stars of low luminosity, i.e. no low-mass ( $M < 3 M_{\odot}$ ) and faint ( $M_{\text{bol}} > -5$ ) carbon stars were predicted to form according to full AGB calculations. He suggested that the problem could be partially alleviated if the onset of the dredge-up episodes occurs much earlier during the TP-AGB evolution of low-mass stars. This implies a smaller  $M_c^{\min}$  than found in full calculations (see Table 1). The question was considered by arbitrarily changing the value of the mixing-length parameter, initially set to  $\alpha \sim 1$ . The net result was to lower systematically the minimum total mass for dredge-up at increasing  $\alpha$ , whereas the corresponding  $M_c^{\min}$  was slightly affected. Moreover, it became clear that, for given stellar mass  $M$ ,  $M_c^{\min}$  increases with  $Z$  and, for given  $Z$ , it decreases with  $M$ .

Boothroyd & Sackmann (1988d) also addressed the problem of the formation of low-mass carbon stars by analysing the effect of adopting high values of the mixing length parameter [e.g.  $\alpha \sim 3$  was necessary to produce a  $0.81 M_{\odot}, Z = 0.002$  carbon star with  $M_c \sim 0.566 M_{\odot}$  and a luminosity at the post-flash dip  $\log(L/L_{\odot}) \sim 3.34$ , or equivalently  $M_{\text{bol}} \sim -3.59$ ; see also Table 1]. The authors remarked that the value of  $\alpha$  has a large effect on the depth in temperature of the convective envelope, but it has a relatively small effect on the depth in mass. In fact, the base of the convective envelope is located in a zone containing a very small mass [ $\sim (10^{-4} - 10^{-3})M_{\odot}$ ], but across which the temperature gradient is extremely steep. Moreover, Boothroyd & Sackmann (1988d) concluded that the experiment of varying  $\alpha$ , though useful, cannot definitively solve the problem of dredge-up.

These considerations suggest us the possibility of performing the analysis on the occurrence of third dredge-up from a different perspective, in the sense that we keep the mixing-length parameter fixed at its value ( $\alpha = 1.68$ ) derived from the calibration of the solar model, calculated

with the complete evolutionary code of Padua (Girardi et al. 1996). We specify that the adopted opacities are taken from Iglesias & Rogers (1996; OPAL) in the high-temperature domain ( $T > 10^4 \text{ K}$ ), and from Alexander & Ferguson (1994) in the low-temperature domain ( $T < 10^4 \text{ K}$ ). We analyze, instead, the effect of assuming different values of the characteristic temperature for dredge-up. The lower  $T_b^{\text{dred}}$ , the smaller is the value  $M_c^{\min}$ . To this respect, we can safely state that increasing  $\alpha$  produces the same effect on  $M_c^{\min}$  as decreasing  $T_b^{\text{dred}}$ .

The reasons why we opt for such a choice are the following. First, we want to secure the continuity of the TP-AGB calculations with the previous evolution, entirely followed using  $\alpha = 1.68$ . This does not mean at all that in reality the efficiency of the convective mixing cannot change during the evolution of the star. However, since the present theoretical treatment of the convection is indeed inadequate to predict possible variations of  $\alpha$ , we prefer to assume a conservative position. Second, the occurrence of convective dredge-up is not only conditioned by the properties of external convection (e.g. by the choice of  $\alpha$ ), but it also depends on the physical characteristics of the inter-shell region directly involved in the flash. Detailed calculations clearly indicate that a higher strength of the pulse, (usually measured by the maximum luminosity of the He-shell) corresponds to a greater amount of energy spent to expand outward the nuclearly processed material, that would be cooled down more efficiently (Boothroyd & Sackmann 1988d; Straniero et al. 1997).

Therefore, artificially decreasing  $T_b^{\text{dred}}$  is equivalent to hypothesising stronger thermal pulses. This is a viable experiment in a theoretical approach making use of a static envelope model. In fact, our analysis is not directed to investigate the effective penetration of the convective envelope, since that would require us to carefully follow (i.e. with a complete stellar code) the onset and the time development of each thermal pulse. Obviously, an impossible task using only envelope integrations. The essential goal of this study is to simply derive useful indications on the possible occurrence of convective dredge-up, on the basis of physical aspects which can be properly handled by our investigative tool.

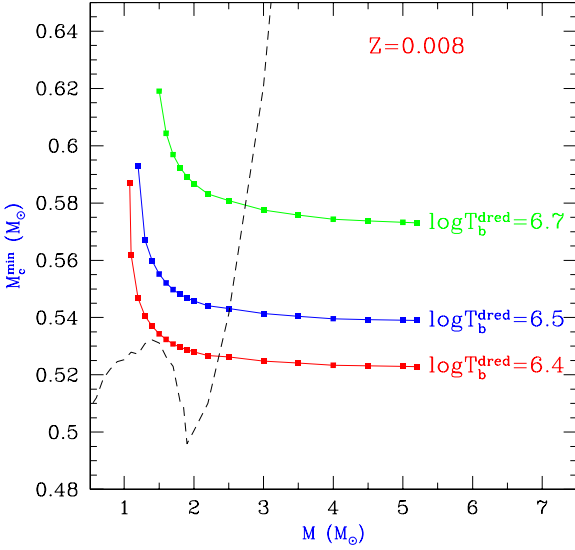


**Fig. 2.** Minimum core mass for dredge-up,  $M_c^{\min}$ , as a function of the current stellar mass for models with  $[Y = 0.25, Z = 0.008]$ , corresponding to three values of  $T_b^{\text{dred}}$ . The short-dashed line refers to the core mass at the first thermal pulse.

### 3.3.3. The dependence of $M_c^{\min}$ on $M$ and $Z$

In this section we aim at investigating the dependence of  $M_c^{\min}$  on the stellar mass  $M$  and metallicity  $Z$ , for different values of the temperature parameter  $T_b^{\text{dred}}$ .

As starting point, we explore both the cases  $\log T_b^{\text{dred}} = 6.7$  (from Wood 1981) and  $\log T_b^{\text{dred}} = 6.5$  (following Boothroyd & Sackmann 1988d) to calculate  $M_c^{\min}$  as a function of the stellar mass for the set of models with original composition  $[Y = 0.250, Z = 0.008]$ . The results are displayed in Fig. 2, together with the case  $\log T_b^{\text{dred}} = 6.4$ .

One can immediately notice that all three curves share a common trend, i.e.  $M_c^{\min}$  very steeply increases toward lower masses [ $M < (1.5 - 1.8)M_\odot$ ], and flattens out to a nearly constant value for greater masses ( $M > 2M_\odot$ ). The comparison of these curves with the values of the core mass at the starting of the thermally pulsing regime (short-dashed line) allows one to get an approximate estimate of the core-mass increment necessary before the star begins to become carbon-enriched. It turns out that stars with masses  $M > 2.5M_\odot$  enter the TP-AGB phase with a core mass that is greater than the corresponding  $M_c^{\min}$ , for all the three values of temperature  $T_b^{\text{dred}}$  under study, i.e. the third dredge-up should already occur at the first pulse (or, more likely, as soon as the full-amplitude regime is established). On the contrary, stars with lower masses ( $M < 2.5M_\odot$ ) are expected to evolve through a

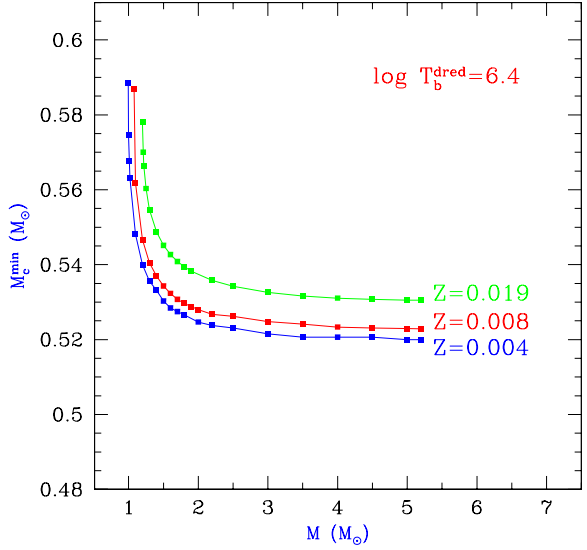


**Fig. 3.** Minimum core mass for dredge-up,  $M_c^{\min}$ , as a function of the current stellar mass for models with metallicity  $Z = 0.004, Z = 0.008$ , and  $Z = 0.019$ , corresponding to the indicated value of  $\log T_b^{\text{dred}}$ .

longer part of the TP-AGB without undergoing any chemical pollution by convective dredge-up.

Moreover, it is worth noticing that each possible choice of  $T_b^{\text{dred}}$  determines a different value of the minimum total mass,  $M_{\text{dred}}^{\min}$ , for a star to experience dredge-up. In the  $Z = 0.008$  case, calculations yield  $M_{\text{dred}}^{\min} \sim 1.5M_\odot$  adopting  $\log T_b^{\text{dred}} = 6.7$ ,  $M_{\text{dred}}^{\min} \sim 1.2M_\odot$  adopting  $\log T_b^{\text{dred}} = 6.5$ , and  $M_{\text{dred}}^{\min} \sim 1.1M_\odot$  adopting  $\log T_b^{\text{dred}} = 6.4$ .

The dependence on metallicity is illustrated in Fig. 3, for a fixed value of  $\log T_b^{\text{dred}} = 6.4$ . In agreement with the results from full computations of thermal pulses (e.g. Boothroyd & Sackmann 1988d), our analysis confirms that for given stellar mass, the onset of convective dredge-up is favoured at lower metal abundances in the envelope. It is worth noticing that the minimum mass,  $M_{\text{dred}}^{\min}$ , is affected in the same direction. According to our calculations, we get  $M_{\text{dred}}^{\min} \sim 1.2M_\odot$  for  $Z = 0.019$ ,  $M_{\text{dred}}^{\min} \sim 1.1M_\odot$  for  $Z = 0.008$ , and  $M_{\text{dred}}^{\min} \sim 1M_\odot$  for  $Z = 0.004$ . This result seems to be consistent with the observed data of carbon stars in the Magellanic Clouds (see Sect. 4): the faint end of the luminosity distribution of carbon stars in the SMC (with a mean metallicity  $Z \sim 0.004$ ) extends to a fainter luminosity ( $M_{\text{bol}} \sim -2.5$ ), than in the LMC ( $M_{\text{bol}} \sim -3$ , with a mean  $Z \sim 0.008$ ), thus suggesting a lower  $M_{\text{dred}}^{\min}$  at lower metallicities.

We like to stress once more that the onset of the mixing events in low-mass stars is a fundamental aspect, since it crucially affects the distribution of the carbon stars in the low-luminosity domain. As will be shown below (from



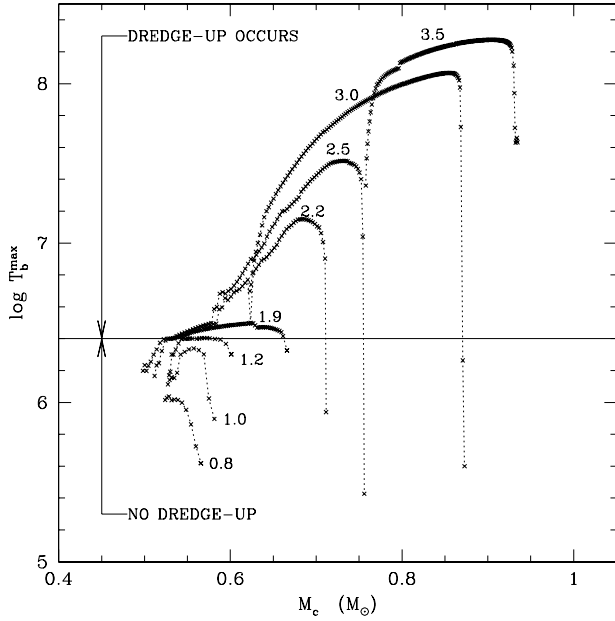


**Fig. 4.** Maximum base temperature,  $T_b^{\max}$ , calculated at each thermal pulse (crosses connected by dotted lines) as a function of the core mass for a few evolving TP-AGB stellar models with original metallicity,  $Z = 0.008$ . Stellar masses at the onset of the TP-AGB phase are indicated in solar units nearby the corresponding curves. The solid horizontal line marks the critical temperature ( $\log T_b^{\text{dred}} = 6.4$ ) for the occurrence of the third dredge-up.

a systematic analysis), the value  $\log T_b^{\text{dred}} = 6.4$  is found suitable to fulfill the above constraint (Sect. 4) in the Magellanic Clouds.

It is worth specifying that the results illustrated in Fig. 2 give  $M_c^{\text{min}}$  as a function of the *current total mass* (not the mass at the first thermal pulse). This is particularly relevant in the low-mass domain, where the curves become very steep, i.e. minor variations of the total mass correspond to quite different values of  $M_c^{\text{min}}$ . Since TP-AGB calculations are performed with the inclusion of mass loss by stellar winds, it follows that *in the case of low-mass stars a small reduction of the envelope mass may significantly delay, or even prevent the onset of dredge-up.*

Figure 4 shows the maximum temperature at the base of the convective envelope,  $T_b^{\max}$ , at the stage of post-flash luminosity peak, as a function of the core mass during the evolution of a few stellar models with different masses  $M$  at the beginning of the TP-AGB phase, and original metallicity  $Z = 0.008$  (see Sect. 3.5 for further details of the models). The adopted temperature parameter is  $T_b^{\text{dred}} = 6.4$ .

Envelope integrations indicate that if the envelope mass is too small, the star fails to attain the minimum temperature  $T_b^{\text{dred}}$ , whatever the core mass is. See, for instance, the track for the  $M = 0.8M_\odot$  star. The model with

$M = 1.2M_\odot$  corresponds to the lowest mass for a star to become carbon-enriched. Higher mass stars are able to attain hot base temperatures, so that they are expected to experience dredge-up already since the first pulses.

The present method also provides the possibility of predicting the stage beyond which dredge-up cannot occur any longer during the final TP-AGB evolution. The shut-down of dredge-up may happen when the envelope mass becomes so small that the condition  $T_b^{\max} \geq T_b^{\text{dred}}$  is no longer satisfied. This circumstance occurs for the last pulses of the tracks displayed in Fig. 4, characterized by the drastic reduction of the envelope mass due to stellar winds. This point represents another important improvement for synthetic TP-AGB models, since the end of the dredge-up episodes is not fixed a priori (a necessary assumption if one adopts a constant value for  $M_c^{\text{min}}$ ), but naturally derives from calculations.

### 3.4. The inter-shell chemical composition

The remaining ingredient of our models is the composition of the dredged-up material. We use the same formalism as in Marigo et al. (1996a), to whom we refer for an extensive description of this point. Suffice it to recall that our prescription is based on the detailed calculations of the inter-shell nucleosynthesis carried out by Boothroyd & Sackmann (1988c). They find that the convective inter-shell after a thermal pulse and just before the penetration of the envelope is composed by 20 – 25 % of  $^{12}\text{C}$ ,  $\sim 2$  % of  $^{16}\text{O}$ , and the remainder of  $^4\text{He}$  (in mass fractions). These proportions are reached after the first few thermal pulses, and do not significantly depend on the core mass and metallicity.

Recently, Herwig et al. (1997) have pointed out that the abundances in the inter-shell will differ significantly from the results of standard calculations (i.e. without extra-mixing as in Boothroyd & Sackmann 1988c), if instead one applies their overshooting scheme to all convective zones. The resulting chemical distribution of the dredged-up material typically consists of 50% in  $^{12}\text{C}$ , 25% in  $^{16}\text{O}$ , and 25% in  $^4\text{He}$ .

In this study we opt for the conservative standard prescription of Boothroyd & Sackmann (1988c). The following fixed abundances are adopted: 22% for  $^{12}\text{C}$  produced by the triple alpha reaction and 2% for  $^{16}\text{O}$  produced by the reaction  $^{12}\text{C}(\alpha, \gamma)^{16}\text{O}$ .

### 3.5. Other computational details

The evolutionary calculations presented in this study have been carried out for a dense grid of stellar masses ( $0.8M_\odot \lesssim M_i \lesssim 5M_\odot$ ) and two values of the initial metallicity,  $Z = 0.008$  and  $Z = 0.004$ . In addition to the new treatment of the third dredge-up already presented, the present calculations are based on a synthetic TP-AGB model, having the same general structure as described

in Marigo et al. (1996a), with some major revisions and updates illustrated in Marigo et al. (1998) and Marigo (1998ab). The reader should refer to these works for all the details. Suffice it to recall here that the synthetic model combines analytical relations with a complete stellar envelope, which is integrated from the photosphere down to the core. The evolution of a TP-AGB star is followed from the first thermal pulse up to the complete ejection of the envelope, adopting the prescription for mass loss as suggested by Vassiliadis & Wood (1993). A homogeneous set of accurate analytical relations (e.g. the core mass-luminosity relation, the core mass-interpulse period) is taken from the recent work by Wagenhuber & Groenewegen (1998). Finally, it is worth remarking that the occurrence of envelope burning (or hot-bottom burning) in more massive TP-AGB stars ( $M \gtrsim 3.5M_{\odot}$ ) is consistently followed to account for the possible break-down of the  $M_c - L$  relation (see Marigo 1998b).

#### 4. The observed carbon star luminosity functions in the MCs

The Magellanic Clouds – LMC and SMC – are an ideal site for testing evolutionary theories of AGB stars, thanks to the fortunate combination of several factors:

- The extinction to both Clouds is low and relatively uniform.
- The galaxies are far enough ( $\sim 50$  kpc to the LMC,  $\sim 63$  kpc to the SMC) that their depth along the line of sight can be neglected to first order, and the same distance can be assigned to all the stars.
- At the same time the galaxies are near enough to allow the resolution and analysis of single stellar sources by means of both photometric and spectroscopic techniques.
- Both Clouds have a considerable number of populous star clusters whose age (Elson & Fall 1985; Girardi et al. 1995) and chemical composition (Olszewski et al. 1991) can be estimated with a good accuracy, and which contain a considerable number of AGB stars (Frogel et al. 1990; Westerlund et al. 1991).
- A large amount of observed data on AGB stars is nowadays available (see the reviews by Westerlund 1990 and Groenewegen 1997), thanks to large scale surveys ranging from the optical to the radio domain, and spectroscopic analyses for the estimation of stellar parameters (e.g. effective temperature, mass-loss rate, wind velocity, surface gravity, surface chemical abundances).

For the observed carbon star luminosity function in the LMC we make use of the recent compilation of Costa & Frogel (1996). The data refer to 895 carbon stars, selected among the original sample of 1035 stars found by Blanco et al. (1980) and Blanco & McCarty (1983) by means of low-dispersion red grism spectroscopy in 52 fields of the

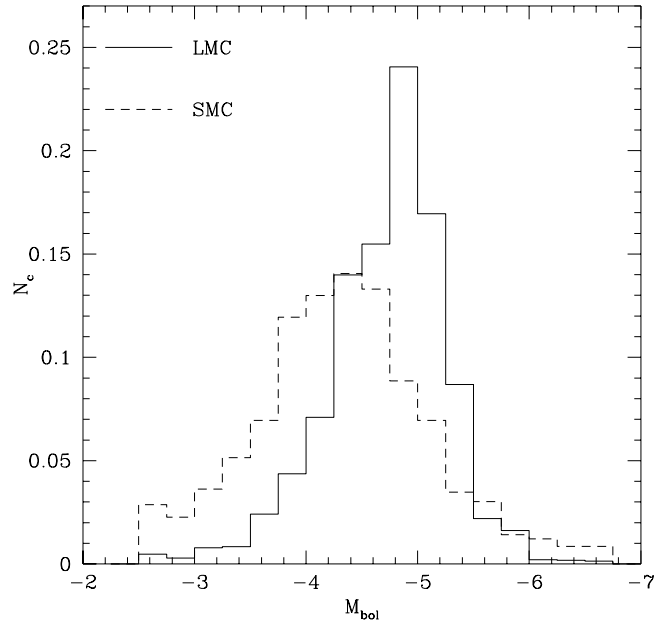


**Fig. 5.** The observed LFs of carbon stars detected in the fields of the LMC (solid line) and SMC (dashed line), normalised to the total number of stars in the samples. The data for the LMC are taken from Costa & Frogel (1996), adopting a distance modulus  $\mu_0 = 18.5$ . The data for the SMC is as derived by Groenewegen (1997) from the data compiled by Rebeiro et al. (1993), with a distance modulus  $\mu_0 = 19.0$ .

galaxy, distributed over an area of  $8^\circ \times 8^\circ$ . The identification of carbon stars was based on the recognition in stellar spectra of a typical blend of the CN bands at near-infrared wavelengths ( $\lambda\lambda 7910, 8100, 8320$ ). It is worth remarking that this sample of carbon stars can be considered almost complete and not limited by apparent magnitude, since the faintest carbon stars are at least 2 mag brighter ( $I \sim 15$ ) than the faint limit of detection ( $I \sim 17$ ). Moreover, the possible contribution of high luminosity carbon stars, which would have been missed in the survey because of dust obscuration, is likely to be rather small ( $\lesssim 3\%$  for  $M_{\text{bol}} < -6$  according to Groenewegen & de Jong 1993). Costa & Frogel (1996) performed *RI* and/or *JHL* photometry of the selected 895 carbon stars. The apparent bolometric magnitudes  $m_{\text{bol}}$  were estimated first applying proper bolometric corrections to the *K* magnitude of a subsample of stars with available *JHK* photometry. On the basis of these results the authors derived a linear relationship, expressing  $(I_0 - m_{\text{bol}})$  as a function of the red colour  $(R - I)_0$ , which was then used to obtain  $m_{\text{bol}}$  for the majority of carbon stars with only *RI* data. The authors quoted a mean error on the evaluation of  $m_{\text{bol}}$  of approximately  $\pm 0.34$  mag.

The observed CSLF in the LMC is plotted in Fig. 5 (solid line). The absolute bolometric magnitudes,  $M_{\text{bol}}$ ,

are obtained from the apparent ones adopting a distance modulus  $\mu_0 = m_{\text{bol}} - M_{\text{bol}} = 18.5$ , as indicated by Westerlund (1990) and favoured by several recent works (e.g. Wood et al. 1997; Oudmaijer et al. 1998; Madore & Freedman 1998; Salaris & Cassisi 1998; Panagia 1998).

The resulting CSLF is quite similar to those obtained from previous samples of carbon stars in the fields of the LMC (Westerlund et al. 1978; Richer et al. 1979; Cohen et al. 1981). It extends approximately from  $M_{\text{bol}} = -3$  up to  $M_{\text{bol}} = -6.5$ , with the peak located at around  $M_{\text{bol}} = -4.875$  (centre of the bin). The dispersion of the observed distribution is estimated to be about  $\sigma = 0.55$  mag.

From a comparison with the CSLF in selected clusters of the LMC (Frogel et al. 1990) it turns out that the two distributions are quite similar, except for few subtle differences, namely, the presence of somewhat more extended faint and bright tails in the field distribution relative to that of the clusters. According to Marigo et al. (1996b), the explanation of this resides in the presence of two different periods of quiescence in the cluster formation history of the LMC, shaping the age (and progenitor mass) distribution of C stars. These gaps are found at ages of  $\sim (3 - 12) \times 10^9$  yr, and  $\sim (2 - 6) \times 10^8$  yr (see also Girardi et al. 1995), which roughly correspond to the ages of the least ( $\sim 1.2M_{\odot}$ ) and most ( $\sim 4M_{\odot}$ ) massive carbon star progenitors, respectively.

Figure 5 also shows the observed CSLF in the SMC (dashed line), as derived by Groenewegen (1997) from a sample of 1636 stars observed by Rebeiro et al. (1993). The adopted bolometric correction are those by Westerlund et al. (1986). The adopted distance modulus for the SMC is  $\mu_0 = 19.0$  (see Westerlund 1990 for a review of SMC distance determinations).

The first bin of this CSLF contains all stars fainter than  $M_{\text{bol}} = -2.5$ . They are less than 3 % of the total sample of SMC carbon stars. Their intrinsic magnitudes can be as low as  $M_{\text{bol}} = -1.8$ , as found by Westerlund et al. (1995). The formation of carbon stars at such low luminosities can hardly be understood as the result of the third dredge-up in single AGB stars. Most probably, they arise from the evolution in close binary systems (see e.g. de Kool & Green 1995; Frantsman 1997), in which the surface of a low-mass star has been contaminated by the ejecta of a former AGB star companion. The low-luminosity carbon stars will not be considered in this work, since we are dealing with single star evolution. For all practical comparisons, we will consider the CSLF in the SMC as extending down to  $M_{\text{bol}} = -2.5$ .

The CSLFs are significantly different in the two Magellanic Clouds. In the SMC the CSLF is much broader, and presents a fainter peak location (at  $M_{\text{bol}} \sim -4.375$ ; centre of the bin) than that in the LMC ( $M_{\text{bol}} \sim -4.875$ ). This indicates that LMC carbon stars are, on the mean, about 60 % brighter than their SMC counterparts. As remarked by Groenewegen (1997), explaining this difference quan-

titatively represents a challenge for synthetic TP-AGB models.

## 5. The theoretical carbon star luminosity function

In order to simulate the observed CSLF in the Magellanic Clouds, we employ the general scheme already used in Marigo et al. (1996a). For the sake of completeness, we here simply recall the basic steps.

Dividing the luminosity range of interest (e.g.  $-2.5 > M_{\text{bol}} > -7.0$ ) into a suitable number of intervals, for each  $k^{\text{th}}$  luminosity bin of width  $\Delta M_{\text{bol}}$ , we are required to evaluate the number  $N_k$  of carbon stars which are expected to be in transit at the present epoch:

$$N_k = \int_{M_i^{\text{min}}}^{M_i^{\text{max}}} N_k(M_i) dM_i \propto \int_{M_i^{\text{min}}}^{M_i^{\text{max}}} \Phi(M_i, t) \Delta\tau_k(M_i) dM_i \quad (9)$$

where  $\Phi(M_i, t)$  is the stellar birth rate, i.e. the number of stars formed with mass  $M_i$  at the epoch  $t$ , per unit of mass and time (see Sect. 5.1); and  $\Delta\tau_k(M_i)$  is the time each star of mass  $M_i$  spends in the  $k^{\text{th}}$  luminosity interval. Thus,  $N_k(M_i)$  expresses the number of carbon stars evolved from a progenitor with initial mass  $M_i$  and a current (i.e. at the present time) luminosity inside the  $k^{\text{th}}$  bin.

The integration is performed over the mass range  $[M_i^{\text{min}}, M_i^{\text{max}}]$ . We denote with  $M_i^{\text{min}}$  the maximum of the lower mass limit for the formation of carbon stars and the mass of the star whose lifetime is just the age of the galaxy ( $\sim 0.87M_{\odot}$  for  $T_G = 15$  Gyr). We refer to  $M_i^{\text{max}}$  as the minimum of the upper mass limit for carbon star formation, and the maximum mass of stars which experience the AGB phase,  $M_{\text{up}}$ . In our case, the evolution of the progenitor stars has been calculated with the adoption of an overshoot scheme applied to the convective zones, from the ZAMS up to the starting of the TP-AGB (Girardi et al. 1998). The overshooting parameter for core convection adopted for intermediate-mass stars ( $\Lambda_c = 0.5$ ) characterises a moderate efficiency for this process. This fixes  $M_{\text{up}} \simeq 5M_{\odot}$ . Classical models without overshoot would predict a higher value, e.g.  $M_{\text{up}} \sim (7 - 8)M_{\odot}$ .

Let us now discuss the meaning of the two basic functions in Eq. (9), namely  $\Phi(M_i, t)$  and  $\Delta\tau_k(M_i)$ .

### 5.1. The stellar birth rate

It is useful to split the stellar birth rate  $\Phi$  into the product of two functions (see Tinsley 1980):

$$\Phi(M_i, t) = \phi(M_i) \psi(t) \quad (10)$$

where  $\phi(M_i)$  is the initial mass function (IMF) expressing the fraction of stars forming with masses in the range  $[M_i, M_i + dM_i]$ . This latter is normalised so that:

$$\int_0^{\infty} M_i \phi(M_i) dM_i = 1 \quad (11)$$

In this work we adopt the classical power-law IMF of Salpeter (1955),  $\phi(M_i) \propto M_i^{-(1+x)}$ , with  $x = 1.35$ . The function  $\psi(t)$  is the star formation rate (SFR) and represents the mass of primordial gas that is converted into stars per unit of time at the epoch  $t$ .

In the particular case under consideration [see Eq. (9)], it is required to evaluate the number of carbon stars with initial mass  $M_i$  and lifetime  $\tau^*$  which are born at the epoch  $t = T_G - \tau^*$  (and hence are presently observable), where  $T_G$  is the age of the galaxy. This can be expressed by:

$$\Phi(M_i, T_G - \tau^*) = \phi(M_i) \psi[T_G - \tau^*(M_i)] \quad (12)$$

Since there is a unique correspondence between the lifetime of a star (of given metallicity) and its initial mass,  $\tau^* = \tau^*(M_i)$ , it is possible to consider  $\Phi$  as a function solely of the stellar mass.

### 5.2. The rate of brightening

The quantity  $\Delta\tau_k(M_i)$  is the time that a star with initial mass  $M_i$  spends in the  $k^{\text{th}}$  luminosity bin of width  $\Delta M_{\text{bol}}$ . It is directly derived from the TP-AGB evolutionary tracks.

A useful approximation for interpreting the results is that the quiescent luminosity of TP-AGB stars follows an almost constant rate of brightening (see e.g. Iben 1981):

$$\frac{dM_{\text{bol}}}{d\tau} \sim \text{constant} \quad (13)$$

Actually, this relation holds if the following conditions are met. First, the relation between the quiescent luminosity  $L$  and the core mass  $M_c$  should be linear. This would correspond to consider only the terms (5a) and (5b) of Eq. (5) giving the  $M_c - L$  relation adopted by Marigo (1998b). This implies the neglect of both the initial sub-luminous evolution of the first inter-pulse periods, and the possible deviations towards higher luminosities caused by envelope burning. This assumptions are reasonable for carbon stars since their formation generally occurs after the onset of the full amplitude regime, and only when envelope burning is not efficiently operating. In this case:

$$\frac{dM_c}{dL} = K_1 \quad (14)$$

On the other hand, the evolutionary rate (i.e. the growth rate of the core mass) is proportional to the stellar luminosity:

$$\frac{dM_c}{d\tau} = K_2 \frac{L}{X} \quad (15)$$

In the above equations  $K_1$  and  $K_2$  are suitable constants. If the changes in the envelope abundance of hydrogen,  $X$ , are small enough, it follows that  $dM_c$  can be eliminated from the above equations giving  $d \ln L / d\tau = \text{constant}$ , which is equivalent to Eq. (13). This equation tells us that

the *rate of brightening* along the TP-AGB is nearly constant, regardless of the core mass, the total mass, and the luminosity level.

In our computations, the rate of brightening for carbon stars is found to be constant within  $\sim 35\%$  at most. Typical values for this quantity are  $\sim -(3.5-7) 10^{-7} \text{mag yr}^{-1}$ . Under these conditions, it follows that nearly the same number of stars is expected to populate each magnitude interval along the AGB phase of coeval (e.g. a cluster) stellar populations. If we consider only the evolution of the quiescent luminosity (see, however, Sect. 5.4 below), the resulting CSLF would be described by a box-like distribution.

A final remark is worth making. Since dredge-up periodically reduces the core mass, then it is expected to affect the average evolutionary rate  $dM_c/d\tau$ . This implies that Eq. (15) is valid only if either dredge-up is not operating, or  $\lambda = \text{constant}$  as in our prescriptions. In contrast, for  $\lambda$  variable with time, neither  $K_2$  nor the rate of brightening  $dM_{\text{bol}}/d\tau$  would be constant.

### 5.3. Transition luminosities

The calculation of the CSLF requires also the knowledge of:

- the luminosities marking the transition from the M-class ( $C/O < 1$ ) to the C-class ( $C/O > 1$ ),
- the maximum luminosities at which the star is still a carbon star,

as a function of the initial mass.

Figures 6 and 7 show the transition luminosities as a function of the initial mass for the  $Z = 0.008$  and  $Z = 0.004$  cases, respectively. The choice of dredge-up parameters adopted to construct these plots will be discussed later in Sects. 6 and 7. Several interesting features can be noticed from the inspection of these figures.

First, the formation of carbon stars may be prevented because of missing or insufficient dredge-up in the range of lower masses, or significantly delayed due to the occurrence of envelope burning in the most massive AGB stars.

Second, for the majority of low-mass carbon stars (with no envelope burning;  $M_i \lesssim 3.5M_\odot$ ; see Marigo 1998b) the maximum luminosity just coincides with the tip of the AGB reached at the end of their evolution. On the contrary, in more massive carbon stars ( $M_i \gtrsim 3.5M_\odot$ ) the occurrence of envelope burning can lead to a different configuration. It may happen that the onset of envelope burning takes place after the star has already experienced a sufficient number of dredge-up episodes to become a carbon star. Nuclear burning at the base of the envelope subsequently destroys carbon, lowering the C/O ratio again below unity. Then, the star is expected to evolve like an oxygen-rich star, until a new transition to the C-class possibly occurs in the very late stages of the evolution. In fact,

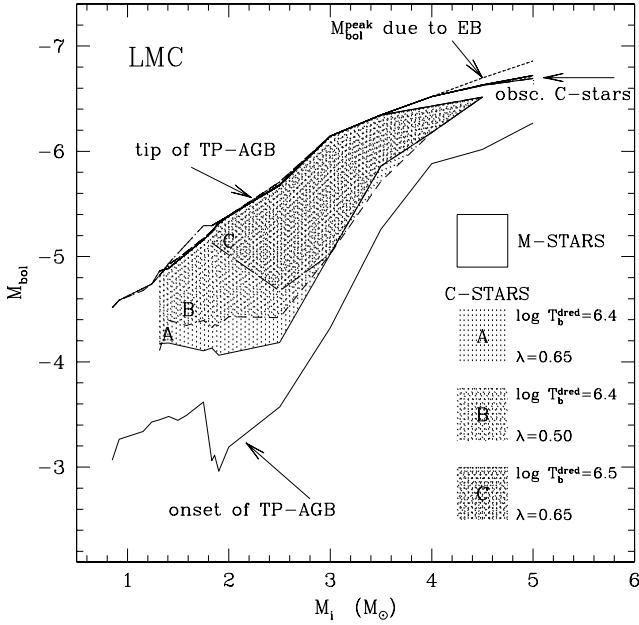


**Fig. 6.** Transition bolometric magnitudes vs. initial masses of TP-AGB stars with original metallicity  $Z = 0.008$ . Regions labelled with letters A, B and C refer to three choices of the dredge-up parameters. See the text for more details.

after envelope burning has extinguished, the star eventually undergoes further convective dredge-up of carbon before leaving the AGB phase (see Frost et al. 1998). Then the star would appear as a carbon star in two distinct evolutionary stages, being oxygen-rich in between. This latter configuration can be clearly noticed in Figs. 6 and 7: at masses higher than about  $3.5M_{\odot}$ , a thin strip indicates the domain of the high-luminosity carbon stars, i.e. those which experienced a late conversion to this spectral type.

In this case, the transition to the carbon star phase may occur under conditions of severe mass-loss. Thus, the brightest carbon stars are expected to be obscured by thick layers of ejected material, then not detectable at visual wavelengths. Actually, high-luminosity obscured carbon stars have been recently discovered in the LMC, by means of infra-red observations (van Loon et al. 1998). Since they are not included in the observed CSLFs in the Magellanic Clouds (Sect. 4), we will not consider them here. The formation of these carbon stars will be investigated by means of the present models in a forthcoming paper.

#### 5.4. The effect of the low-luminosity dip

The fact that low-mass ( $M_i \lesssim 3M_{\odot}$ ) TP-AGB stars undergo a long-lived subluminous stage, soon after the occurrence of a thermal pulse, plays a crucial role in determining the extension of the low-luminosity tail of the

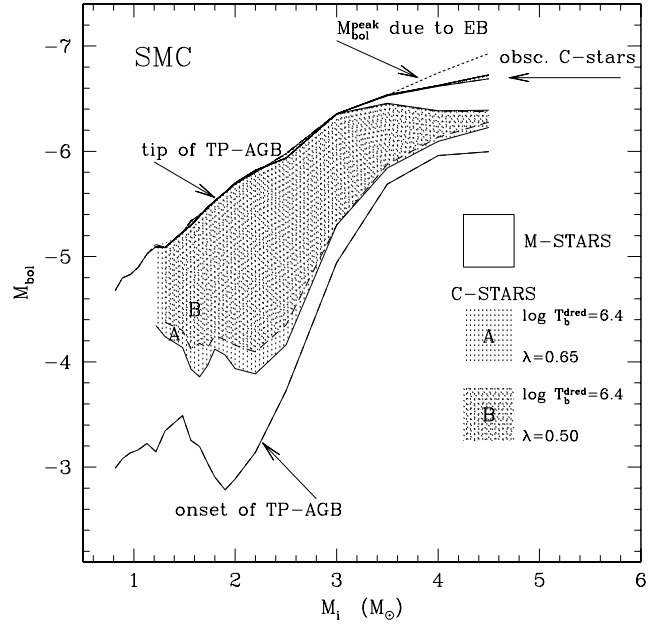


**Fig. 7.** Transition bolometric magnitudes vs. initial masses of TP-AGB stars with original metallicity  $Z = 0.004$ . See the text for more details.

CSLF (Boothroyd & Sackmann 1988ad). It turns out that without accounting for this effect the theoretical distribution cannot extend down to the observed faint end (see also Groenewegen & de Jong 1993), unless quite extreme (and unlikely) assumptions are adopted, e.g. the occurrence of very efficient ( $\lambda \sim 1$ ) dredge-up events since the first weak thermal pulses. On the contrary, the effect of the post-flash luminosity maximum on the CSLF can be neglected, due to its very short duration (Boothroyd & Sackmann 1988a).

In our calculations, the drop in luminosity below the  $M_c - L$  relation is included in a very simple way. On the basis of the results from complete calculations of thermal pulses (Boothroyd & Sackmann 1988a) we construct a function,  $P(L - \Delta L)$ , expressing the probability that a star with quiescent luminosity  $L$ , predicted by the  $M_c - L$  relation, may be found at a lower luminosity level,  $L - \Delta L$ . The maximum excursion towards fainter luminosities is assumed to be  $\Delta \log L = 0.5$ , corresponding to  $\Delta M_{\text{bol}} = 1.25$  mag. The probability function is then estimated for a suitable number of luminosity intervals (5 in our case), with a width equal to the adopted bin resolution, i.e.  $\Delta \log L = 0.1$ , or equivalently  $\Delta M_{\text{bol}} = 0.25$ .

The probability distribution, normalized to unity, is assumed as following:

$$\begin{aligned}
 P_0(\log L) &= 0.35 \\
 P_1(\log L - 0.1) &= 0.28 \\
 P_2(\log L - 0.2) &= 0.20 \\
 P_3(\log L - 0.3) &= 0.10
 \end{aligned} \tag{16}$$

$$P_4(\log L - 0.4) = 0.05$$

$$P_5(\log L - 0.5) = 0.02$$

Then, the number  $N_k$  of carbon stars [see Eq. (9)] predicted to populate the  $k^{\text{th}}$  luminosity bin is calculated according to:

$$N_k = N_{k,0} P_0 + \sum_{i=1}^5 N_{k+i} P_i \quad (17)$$

where  $N_{k,0} P_0$  is the number of objects, following the  $M_c - L$  relation, which are expected to be presently crossing the  $k^{\text{th}}$  interval. The term  $N_{k+i} P_i$  represents the number of stars having higher quiescent luminosity within the  $(k+i)^{\text{th}}$  bin, but presently contributing to the  $k^{\text{th}}$  bin, because of the overlap with the corresponding low-luminosity dip. In other words, the luminosity function derived just applying the  $M_c - L$  relation, is then convolved with the function  $P(L)$  which mimics the shape of the sub-luminous stages driven by thermal pulses.

We have actually adopted the same prescription for all the stars considered, although the duration and the depth of the post-flash luminosity dip are less pronounced in stars of higher core masses (Boothroyd & Sackmann 1988a). Nevertheless, we expect that our approximation does not compromise the validity of the results. This because most of the carbon stars are found in the mass range  $M_i < 2.5M_\odot$ , for which well extended luminosity dips, consistent with Eq. (17), are expected. Moreover, it will be shown in Sect. 6 that these stars completely determine the faint end and peak location of the theoretical CSLFs. More massive AGB stars, instead, are predicted to have less-pronounced luminosity dips. However, they populate mostly the bright wing of the CSLF, which is affected by several other factors (such as the efficiency of envelope burning, mass-loss, and the SFR; see Sect. 6).

## 6. The calibration of the dredge-up parameters for the LMC

The dredge-up parameters,  $T_b^{\text{dred}}$  and  $\lambda$ , need to be calibrated on the basis of some observational constraint. First, we aim at reproducing the CSLF in the LMC, which has already been the subject of previous works (e.g. Groenewegen & de Jong 1993; Marigo et al. 1996a). To this aim, we employ the results of synthetic calculations for TP-AGB stars with initial chemical composition [ $Y = 0.250; Z = 0.008$ ]. The adopted metallicity is in agreement with the observational determinations for the LMC, specially with regard to the young components (e.g. Russell & Dopita 1990; Dopita et al. 1997). Moreover, Olszewski et al. (1991) and de Freitas Pacheco et al. (1998) find similar metallicities in the LMC star clusters younger than about 4 Gyr.

By means of the method outlined in Sect. 5, we have calculated the CSLF for different combinations of the two

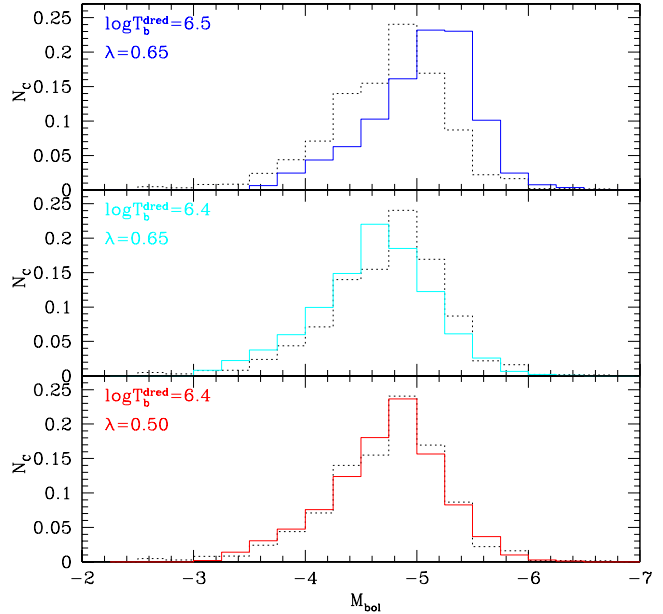


**Fig. 8.** Theoretical luminosity functions of carbon stars (solid lines) for three different combinations of the dredge-up parameters as indicated. The observed distribution in the LMC (dotted line) is plotted for comparison.

parameters, while keeping fixed the other input prescriptions (namely the IMF and SFR). Specifically, we employed Salpeter’s law (1955) for the IMF, and the history of SFR suggested by Bertelli et al. (1992) in their study of the CMDs of field stars in selected areas of the LMC. The SFR has been moderate from the beginning up to about 5 Gyr ago and since then a factor of ten stronger (see the top panel of Fig. 10). The sensitivity of the results to various possible choices of the SFR as a function of the age, and to the assumed IMF, are explored in Sect. 6.3.

In Fig. 8 we show the predicted LF of carbon stars for three pairs of dredge-up parameters. The values are the following:

$$\log T_b^{\text{dred}} = 6.5, \lambda = 0.65$$

$$\log T_b^{\text{dred}} = 6.4, \lambda = 0.65$$

$$\log T_b^{\text{dred}} = 6.4, \lambda = 0.50$$

The corresponding transition luminosities from the oxygen-rich to the carbon-rich domain are plotted as a function of the initial mass in Fig. 6. It is apparent that the formation of carbon stars of lower masses is favoured at decreasing  $T_b^{\text{dred}}$  and increasing  $\lambda$ . On the contrary, the luminosity at the tip of the TP-AGB seems to be essentially independent of the dredge-up parameters (at least for the cases under consideration). A reliable calibration of these parameters requires one to disentangle which distinctive effects are produced by one parameter without the influence of the other. This because it would be desirable

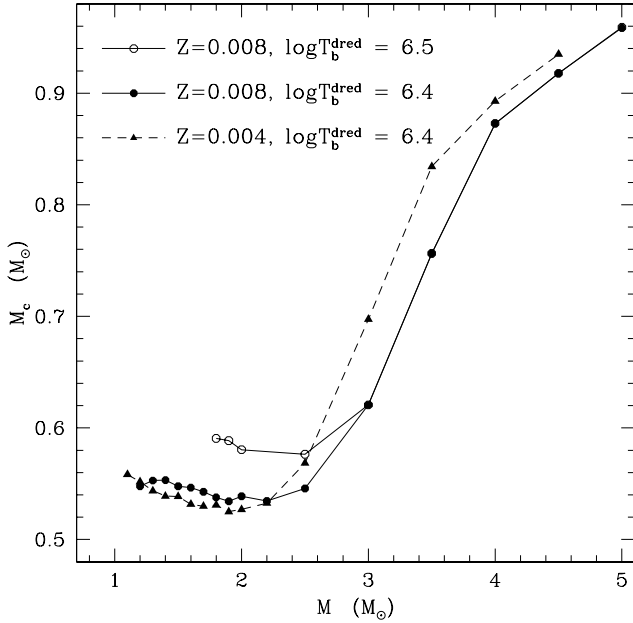


**Fig. 9.** Core mass at the first dredge-up event as a function of the stellar mass at the onset of the TP-AGB phase, for two values of the temperature parameter  $T_b^{\text{dred}}$ , and metallicities  $Z = 0.008$  and  $Z = 0.004$ .

to derive a unique pair of proper values, or at least to reduce the suitable space of parameters as much as possible.

### 6.1. The temperature parameter: $T_b^{\text{dred}}$

Let us first discuss the role of  $T_b^{\text{dred}}$ . We recall that this parameter determines the minimum core mass for dredge-up,  $M_c^{\text{min}}$ , as a function of the stellar mass and metallicity.

In a previous analysis (Marigo et al. 1996a) the reproduction of the CSLF in the LMC was obtained adopting  $M_c^{\text{min}} = 0.58M_\odot$  as a constant parameter, for all stellar masses and chemical compositions (see also Groenewegen & de Jong 1993 for similar results). In contrast, we have shown in Sect. 3.3 that with the new algorithm based on envelope integrations, at fixed  $T_b^{\text{dred}}$  the behaviour of  $M_c^{\text{min}}$  as a function of  $M$  is far from being constant, but steeply increasing for lower values of the mass. Moreover, the onset of the third dredge-up is favoured at lower  $Z$ .

Figure 9 illustrates the core mass – necessarily  $\geq M_c^{\text{min}}$  – just before the occurrence of the first dredge-up episode as a function of the total mass at the starting of the TP-AGB phase for the evolutionary models calculated with initial metallicity  $Z = 0.008$  and  $Z = 0.004$ . The comparison with the previous Fig. 2 shows the following differences.

- First, the core mass at the first dredge-up event does not increase so steeply as  $M_c^{\text{min}}$  in the range of low-mass stars  $M < 2.5M_\odot$ . This is the result of the extreme sensitivity of  $M_c^{\text{min}}$  to the current stellar mass.

**Table 3.** Minimum initial mass,  $M_{\text{min}}^{\text{carb}}$ , of carbon stars’ progenitors, and age of the relative stellar generation for different values of the temperature parameter  $T_b^{\text{dred}}$  and original metallicities. The corresponding mass at the onset of the TP-AGB is also indicated inside parentheses.

$Z$	$\log T_b^{\text{dred}}$	$M_{\text{min}}^{\text{carb}}$	Age (yr)
0.008	6.7	2.00 (2.0)	$1.211 \times 10^9$
	6.5	1.83 (1.8)	$1.514 \times 10^9$
	6.4	1.32 (1.2)	$3.890 \times 10^9$
0.004	6.4	1.13 (1.1)	$5.220 \times 10^9$

Even small reduction of the envelope actually prevents the formation of carbon stars in the steepest part of the curve shown in Fig. 2.

- Second, the core mass at the onset of the third dredge-up is found to increase for stars with  $M \gtrsim 2.5M_\odot$ . In this mass range, it reflects the behaviour of the core mass at the first thermal pulse (which increases with stellar mass), and not the flattening predicted for  $M_c^{\text{min}}$ .
- Finally, the core masses in the low-mass range indicated in Fig. 9 are somewhat larger than the corresponding ones shown in Fig. 2. The reason is partly due to the fact that the results illustrated in this latter plot are derived from calculations in which  $L_P = L_{(P, \text{full})} + \Delta L_{(P, \text{first})}$  (see Sect. 3.1), whereas the term  $\Delta L_{(P, \text{first})}$  has been neglected in the envelope integrations performed to construct Fig. 2. This simplification was adopted because  $\Delta L_{(P, \text{first})}$  contains a dependence on the core mass at the first thermal pulse [see Eq. (3)], whereas at that stage we simply aimed at deriving the behaviour of  $M_c^{\text{min}}$  as a function of the current stellar mass. The neglect of  $\Delta L_{(P, \text{first})}$  leads one to overestimate  $L_P$  for a given core mass, thus yielding slightly lower values of  $M_c^{\text{min}}$ .

Comparing the curves for the same  $\log T_b^{\text{dred}} = 6.4$  and metallicities  $Z = 0.008$  and  $Z = 0.004$ , it turns out that at decreasing metallicity the core mass at the first dredge-up episode is smaller in the low-mass range ( $M \lesssim 2.2M_\odot$ ), whereas it is larger at higher stellar masses ( $M \gtrsim 2.2M_\odot$ ). This is explained as following. The fact that at lower metallicities the minimum base temperature for dredge-up is attained at lower values of  $L_P$  (and hence  $M_c$ ) is only relevant in the low-mass domain, since the onset of the third dredge-up at larger stellar masses essentially reproduces the trend of the core mass at the first thermal pulse, which actually increases at decreasing metallicities for given stellar mass.

Moreover, if we now compare the two curves plotted in Fig. 9, for two values of  $T_b^{\text{dred}}$  and the same  $Z = 0.008$ , it turns out that the temperature parameter determines the minimum mass for a TP-AGB star to experience chemical pollution by convective dredge-up. The lower is  $T_b^{\text{dred}}$

the lower is this limit mass. Then, for a given mass-loss prescription applied to the previous evolution (i.e. during the RGB and part of the AGB up to the onset of dredge-up), we can derive the corresponding stellar mass at the ZAMS. In other words,  $T_b^{\text{dred}}$  fixes a lower limit to the minimum initial mass,  $M_{\text{min}}^{\text{carb}}$ , for a star to become a carbon star, and hence an upper limit to the oldest age of the stellar population possibly contributing to the observed distribution (see Table 3).

Another interesting point to be stressed is that the results shown in Fig. 9 are determined by the temperature parameter only (since  $\lambda$  cannot have any effect prior to dredge-up). This fact allows us to predict already that the value  $\log T_b^{\text{dred}} = 6.5$  should be ruled out, otherwise we would miss the low-luminosity tail of the LMC CSLF. Let us consider the minimum (with  $M_c = 0.577M_\odot$ ) of the corresponding curve in Fig. 9, referring to a star with  $M = 2.5M_\odot$ . Even in the most favourable (but quite unlikely) hypothesis, that the transition to the C-class occurs soon after the first dredge-up episodes (this would require  $\lambda \sim 1$ ), the corresponding luminosity derived from the  $M_c - L$  relation would be  $\log(L/L_\odot) \sim 3.706$ . This is equivalent to  $M_{\text{bol}} \sim -4.564$ , and even adding 1.25 mag (i.e. the typical depth of the low-luminosity dip; see Sect. 5.4), we get a value that is more than  $\sim 0.3$  mag brighter than the observed faint end of the distribution for the LMC, at  $M_{\text{bol}} \sim -3$ .

In the case of  $\log T_b^{\text{dred}} = 6.4$ , the minimum of the curve is at  $M = 1.8M_\odot$ , with  $M_c = 0.538M_\odot$ . Applying the same reasoning, we would obtain the faintest carbon stars at  $M_{\text{bol}} \sim -2.795$ . The latter value is consistent with observed faint end of the CSLF in the LMC.

Even if a full discussion on the carbon star transition luminosity as a function of the stellar mass cannot be developed without considering the combined effect of  $T_b^{\text{dred}}$  and  $\lambda$ , we can conclude from the previous analysis that *the temperature parameter,  $T_b^{\text{dred}}$ , mainly determines the faint end of the CSLF.*

### 6.2. The efficiency parameter: $\lambda$

Let us now analyse the role of the dredge-up efficiency parameter  $\lambda$ . We remind that  $\lambda = 0.65$  was the suitable value estimated by Marigo et al. (1996a) such that, together with  $M_c^{\text{min}} = 0.58M_\odot$ , the CSLF in the LMC was reproduced. The top and middle panels of Fig. 8 show the theoretical distributions of carbon stars adopting  $\lambda = 0.65$ , for  $\log T_b^{\text{dred}} = 6.5$  and  $\log T_b^{\text{dred}} = 6.4$ , respectively. None of them fits the observed histogram.

In the case with ( $\log T_b^{\text{dred}} = 6.5$ ,  $\lambda = 0.65$ ), the theoretical distribution is systematically shifted to brighter luminosities, with respect to the observed one. The opposite situation is found with the combination ( $\log T_b^{\text{dred}} = 6.4$ ,  $\lambda = 0.65$ ), which produces the peak of the predicted CSLF at a fainter magnitude than observed, with an excess of carbon stars at lower luminosity, and conversely a deficit

in the brighter domain. Note, however, that contrary to the previous result with ( $\log T_b^{\text{dred}} = 6.5$ ,  $\lambda = 0.65$ ), both extremes of the observed distribution are fitted.

This circumstance suggests that we are only required to shift the peak of the histogram into the right luminosity bin. We find that this can be obtained by decreasing the parameter  $\lambda$  while keeping fixed  $\log T_b^{\text{dred}} = 6.4$ , rather than varying the temperature parameter itself. There are two main reasons. First, the constraint set by the faint end of the distribution, which has been already fulfilled with the choice  $\log T_b^{\text{dred}} = 6.4$ , would be violated with a higher value of  $T_b^{\text{dred}}$ . Second, we expect that a suitable decrease of  $\lambda$  could move the peak into the right location, and reproduce the faint tail of the distribution at the same time. In fact, the transition luminosity for a star with a very low-mass envelope ( $\sim 1M_\odot$ ) is only slightly affected by changes of  $\lambda$  (provided that  $\lambda \gtrsim 0.4$ ), since 2 – 3 dredge-up episodes generally suffice to cause the transition to carbon star.

Concluding this discussion, we remark that *once  $T_b^{\text{dred}}$  has been determined, the efficiency parameter  $\lambda$  essentially controls the peak location of the CSLF.* We find that *the best fit to the observed CSLF in the LMC is obtained adopting  $\log T_b^{\text{dred}} = 6.4$  and  $\lambda = 0.5$ .* This fit is shown in the bottom panel of Fig. 8.

### 6.3. Sensitivity to the SFR and IMF

The relative weight of different stellar generations contributing to the observed CSLF is determined by the SFR history in the host galaxy, and by the IMF. In this section, we investigate the sensitivity of the predictions on both functions. Let us first analyse the effect due to the SFR history, while fixing the IMF equal to Salpeter’s (1955) prescription. Then, we explore the sensitivity of the CSLF to different choices of the IMF.

We now address the following questions:

- To what extent is the CSLF sensitive to the underlying SFR ?
- Are there any distinctive features of the CSLF setting constraints on the history of SFR ?
- What is more important in shaping the observed CSLF, the efficiency of the dredge-up process or the time evolution of the SFR ?

First of all, it is clear that the possible indications the CSLF may give on the history of the SFR are restricted to the age interval defined by the minimum and maximum initial mass of the progenitors ( $M_{\text{min}}^{\text{carb}}$  and  $M_{\text{max}}^{\text{carb}}$ , respectively). Specifically, we deal with the age interval ranging from about  $3.9 \times 10^9$  yr down to  $1.1 \times 10^8$  yr, corresponding to stellar lifetimes for  $M_{\text{min}}^{\text{carb}} = 1.32M_\odot$  and  $M_{\text{max}}^{\text{carb}} = 5M_\odot$ , respectively. The lower limit of the mass range is determined by the temperature parameter,  $\log T_b^{\text{max}} = 6.4$  (see Sect. 6.1).



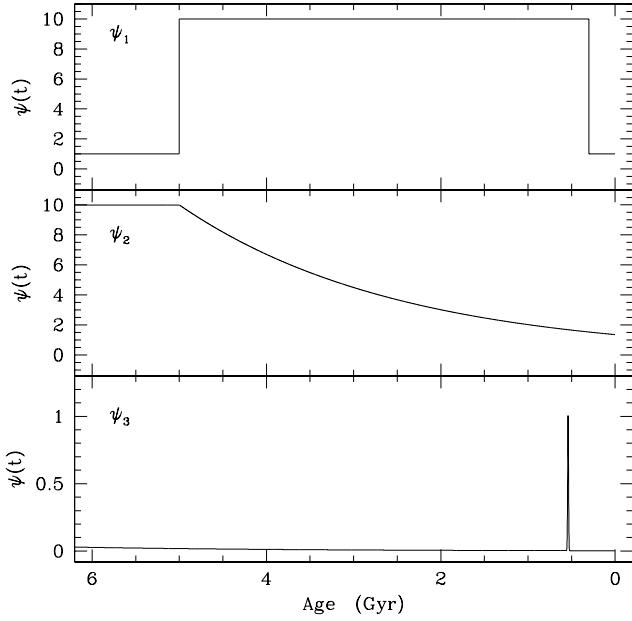


**Fig. 10.** Schematic representation of three different prescriptions for the SFR history in the LMC (in arbitrary units). In the top panel the law suggested by Bertelli et al. (1992) is shown [ $\psi(t) = \psi_1$ ]. See the text for more details.

An interesting result comes out when comparing the theoretical distributions, each corresponding to a single stellar generation, as a function of the initial mass of the progenitor, or equivalently, of the age. These theoretical CSLFs are shown in Fig. 11, for the case  $\log T_b^{\text{dred}} = 6.4$  and  $\lambda = 0.5$ . For each stellar mass (and hence age), the CSLF has a shape determined essentially by the convolution of a box-like function (see Sect. 5.2) with the probability function described in Sect. 5.4. From this figure, it turns out that all the histograms relative to stars with initial masses  $M_i \leq 2.5M_\odot$  have a faint wing extending within the same luminosity range, and more importantly, all the peaks fall into the same bin. This is explained considering that, within this mass range, (i) stars are found to make the transition to the C-class at quite similar luminosities (i.e.  $M_{\text{bol}} \sim -4$ ; see Fig. 6), and (ii) they span as carbon stars a luminosity interval which is comparable to the typical excursion of the low-luminosity dip, i.e.  $\Delta M_{\text{bol}} \sim 1$  mag.

In view of this similarity, we expect that the faint wing of the integrated CSLF is not significantly affected by possible variations in the SFR occurring at ages older than  $\sim 7 \times 10^8$  yr and, in particular, the location of the peak would remain unchanged. On the other hand, differences are evident among the distributions relative to more massive ( $M_i > 2.5M_\odot$ ) carbon stars. Hence, it follows that the high luminosity tail could reflect the details of the recent history of star formation, for ages comprised roughly within  $7 \times 10^8$  and  $10^8$  yr.

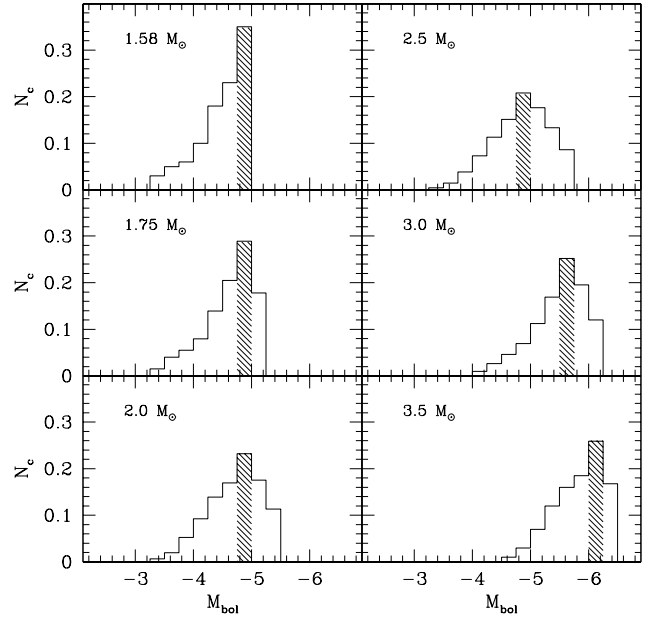


**Fig. 11.** Theoretical CSLFs for simple stellar populations. Each histogram corresponds to the expected distribution of carbon stars of the same age, i.e. evolved from progenitors with the same initial mass, as indicated. The shaded areas mark the position of the luminosity peak for each mass. Notice that all the histograms for  $M_i \leq 2.5M_\odot$  have the peak at the same luminosity bin. Calculations refer to TP-AGB models of initial metallicity  $Z = 0.008$ , for values of the dredge-up parameters,  $\log T_b^{\text{dred}} = 6.4$  and  $\lambda = 0.5$ . Similar behaviours hold for other choices of the parameters.

On the basis of the above considerations, let us now investigate whether it is possible to reproduce the observed CSLF by only varying the adopted SFR, while keeping fixed all the other prescriptions. We start from the theoretical distributions which are found not to fit the observed constraints with our standard prescription for the SFR [ $\psi(t) = \psi_1$ , top panel of Fig. 10], for two different combinations of the dredge-up parameters (top and middle panels of Fig. 8; see also Sects. 6.1 and 6.2).

Concerning the ( $\log T_b^{\text{dred}} = 6.5$ ,  $\lambda = 0.65$ ) case, shown in the top panel of Fig. 8, we can already conclude that the discrepancy cannot be removed, i.e. there is no way to shift the theoretical peak towards lower luminosities. In fact, as previously discussed, the faintest possible location of the peak is characteristic of all simple distributions of carbon stars with initial masses  $\leq 2.5M_\odot$ , corresponding to ages older than  $\sim 7 \times 10^8$  yr. This circumstance makes the lower limit of the peak luminosity almost invariant to any changes in the SFR over this age interval. We can then conclude that *the luminosity location of the peak is indeed a strong calibrator of the efficiency parameter  $\lambda$ .*

Moreover, considering that the extension of the faint tail of the distribution, from the peak down to the end, is essentially controlled by the occurrence of the low-luminosity dip (see Sect. 5.4), it follows that it not possible to populate the observed faintest bins, except by invoking a larger extension of the subluminescent stage (e.g.  $\sim 1.75$  mag) than assumed here (1.25 mag).

Let us now analyse the ( $\log T_b^{\text{dred}} = 6.4$ ,  $\lambda = 0.65$ ) case, illustrated in the middle panel of Fig. 8. We aim at testing whether it is possible to calibrate a suitable law for the SFR, which is able to make the theoretical peak coincide with the observed one and to attain a general agreement of the overall features. After several trials, the best fit is obtained by approximating the SFR as the sum of a decreasing exponential and a gaussian function:

$$\psi(t) \propto \exp\left(-\frac{t}{t_s}\right) + \exp\left[-\frac{1}{2}\left(\frac{t-\bar{t}}{\sigma_t}\right)^2\right] \quad (18)$$

which is illustrated in the bottom panel of Fig. 10 [ $\psi(t) = \psi_3$ ]. The suitable value for the time-scale parameter is  $t_s = 2.5$  Gyr, producing quite a slow decline of the SFR towards younger ages. The effect of the slight decrease is not negligible, as it secures the reproduction of the faint end of the distribution, not reached otherwise with a strictly constant SFR.

The gaussian function, centred at the age  $\bar{t} = 5.5 \times 10^8$  yr and with a standard deviation  $\sigma_t = 0.005$ , mimics the occurrence of a strong and short-lived burst around few  $10^8$  yr ago. This favours the contribution from carbon stars belonging to relatively young stellar generations ( $M_1 \sim 2.8M_\odot$ ), so that the peak of the theoretical distribution is moved into the right luminosity bin. However, it is worth noticing that, although the overall luminosity range fits the observed one, an excess of luminous carbon stars ( $M_{\text{bol}} < -5.25 - -6$ ) is predicted. To get a quantitative estimate of corresponding error we also plot in Fig. 12 the same theoretical distribution, but normalized to the total number of observed carbon stars brighter than  $M_{\text{bol}} = -5.25$ . In this case, the absolute agreement at high luminosities reflects into a considerable deficit of carbon stars fainter than  $M_{\text{bol}} > -5.25$ , covering a fraction of  $\sim 37\%$ , which is considerably smaller than the observed fraction,  $\sim 87\%$ . The mismatch is really significant.

Finally, let us consider the ( $\log T_b^{\text{dred}} = 6.4$ ,  $\lambda = 0.5$ ) case, shown in the bottom panel of Fig. 8, which is the best fit to the observed CSLF in the LMC. The theoretical distribution is obtained adopting a step-wise SFR [ $\psi(t) = \psi_1$  in Fig. 10], that corresponds to the occurrence of a dominant episode of star formation since the age  $t_b = 5 \times 10^9$  yr, up to some more recent epoch  $t_e$ .

In practice, within the significant age range for the formation of carbon stars,  $\psi(t)$  is constant up to  $t_e$ , when the SFR is assumed to suddenly drop to very low (but not zero) values. From our analysis, it turns out that the best agreement with the observed high luminosity tail of

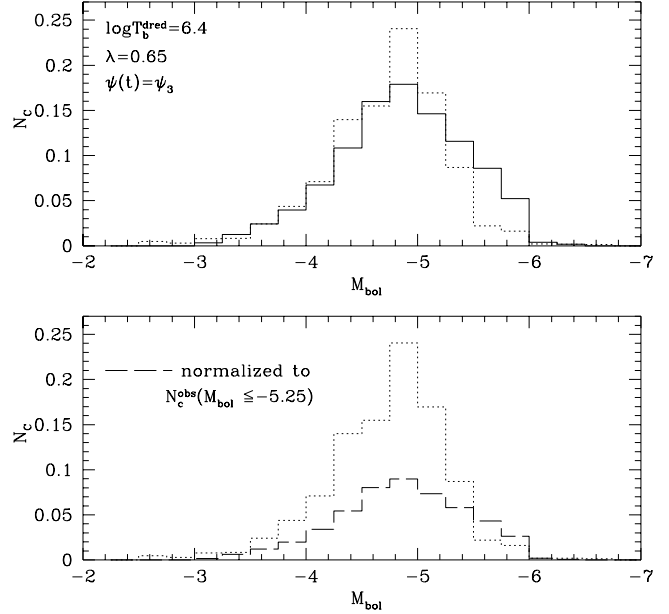


**Fig. 12.** Top panel: the theoretical LF of carbon stars (solid line) obtained with the dredge-up parameters as indicated, and a prescription for the SFR [ $\psi(t) = \psi_3$ ] characterised by a recent burst at around  $5.5 \times 10^8$  yr ago. The dotted line histogram represents the observed LF of carbon stars in the LMC. Bottom panel: The same as in the top panel, but with the theoretical histogram (dashed line) normalised to the number of observed carbon stars more luminous than  $M_{\text{bol}} = -5.25$ .

the distribution ( $M_{\text{bol}} < -5.6$ ) is obtained with  $t_e \sim 5 \times 10^8$  yr. Since the age defining the end of the burst is higher than that of the most massive (i.e.  $4 - 5M_\odot$ ) carbon stars, their contribution remains quite modest, but sufficient to account for the bright end of the distribution at  $M_{\text{bol}} \sim -6.8$ .

If younger ages are assigned to  $t_e$ , a slight excess of luminous carbon stars would show up. In this case, the discrepancy may be removed invoking, instead of a recent sharp decrease in the SFR, a more efficient envelope burning, or stronger mass-loss rates in massive TP-AGB stars. In this respect, it is worth noticing the high luminosity bins of the distribution are crucially affected by the delicate interplay between convective dredge-up, envelope burning, and mass-loss occurring in massive TP-AGB stars. Unfortunately, the present understanding of all these topics is incomplete so that theoretical predictions suffer from a degree of uncertainty.

A further test is performed adopting a SFR law that is slowly decreasing – rather than constant – from an age of 5 Gyr up to now [ $\psi(t) = \psi_2$ , middle panel of Fig. 10]:

$$\psi(t) \propto \exp(-t/t_s) \quad (19)$$

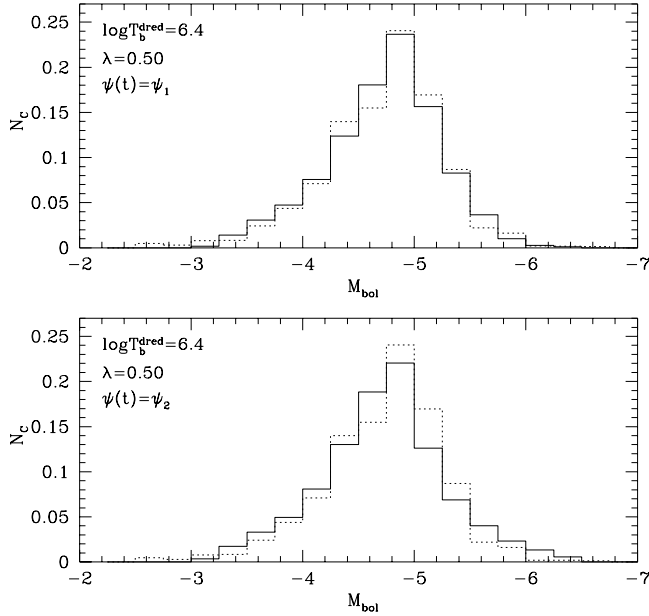


**Fig. 13.** Top panel: the best fit (solid line) to the observed CSLF (dotted line) in the LMC. The theoretical distribution is obtained with the adoption of the dredge-up parameters as indicated, and following the prescription for the SFR ( $\psi(t) = \psi_1$ ) suggested by Bertelli et al. (1992). Bottom panel: The same as in the top panel, but assuming a SFR slowly decreasing with time [ $\psi(t) = \psi_2$ ; see also Fig. 10].

with a time-scale  $t_s = 2.5$  Gyr. The results, shown in Fig. 13, are satisfactory for the faint wing of the distribution, but both the peak and the high luminosity tail are somewhat less well reproduced than with the  $\psi(t) = \psi_1$  prescription.

From the above investigation it follows that *the observed faint tail and the peak location of the CSLF cannot give stringent limits on the history of the SFR, as they are essentially determined by the dredge-up parameters. On the other hand, the bright wing of the distribution is sensitive to the details of the recent SFR.*

Let us now explore the sensitivity of the result to the IMF. In Fig. 14 we present the resulting distributions of carbon stars adopting our best fit for the SFR (i.e.  $\psi_1$  shown in the top-panel of Fig. 10), while varying the law for the IMF according to three choices, namely: Salpeter (1955); Miller & Scalo (1979); and Ferrini et al. (1990). The first two prescriptions for the IMF are empirical, while the third one has a theoretical derivation.

The differences among the predicted luminosity functions are indeed negligible. This can be understood considering that:

- the similarity of the predicted distributions for simple stellar populations with turn-off masses  $1 \lesssim$

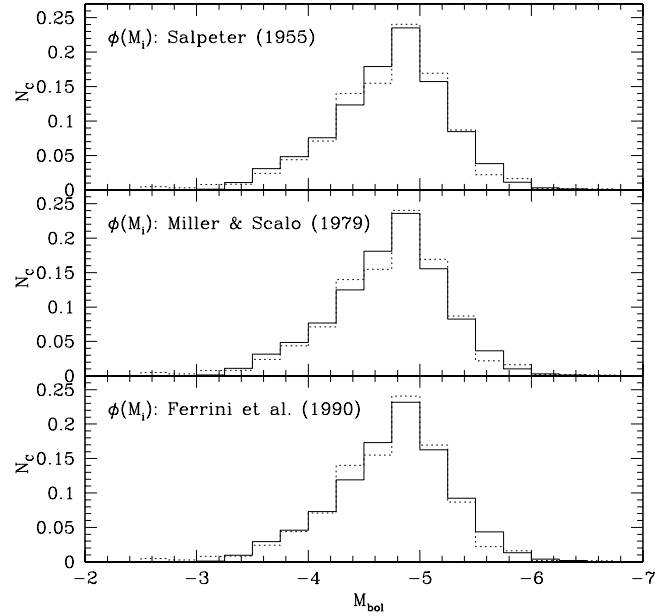


**Fig. 14.** Predicted CSLFs according to different prescriptions for the IMF, as quoted in each panel (solid lines). The dotted line shows the observed distribution in the LMC. The adopted dredge-up parameters are ( $\log T_b^{\text{dred}} = 6.4$ ,  $\lambda = 0.5$ ), and the SFR is  $\psi_1$ .

( $M_i/M_\odot$ )  $\lesssim 2.5$  makes the results quite insensitive to the adopted IMF in this mass range, which indeed provides the major contribution of carbon stars;

- the small weight of the IMF at higher masses tends to cancel the differences in the results obtained with different prescriptions.

In conclusion, *it turns out that the observed distribution of the carbon stars in the LMC is mainly determined by the properties of the third dredge-up (mass-loss, and envelope burning), with the SFR and IMF producing a much weaker effect.*

## 7. The calibration of dredge-up parameters for the SMC

The same kind of procedure described in the previous section is also applied to reproduce the CSLF in the SMC. In this case, we made use of synthetic calculations for TP-AGB stars with initial chemical composition [ $Y = 0.240$ ;  $Z = 0.004$ ]. This values are consistent with present data for the abundances of young populations in the SMC. However, it is also found that the SMC clusters present a clear age–metallicity relation (Da Costa & Hatdizimitriou 1998), with older clusters being systematically more metal poor. If we adopt the mean age–metallicity relation defined by the latter authors (i.e. excluding the apparently abnormal clusters L 113 and NGC 339), we find that it is necessary to go to ages as old as 5 Gyr

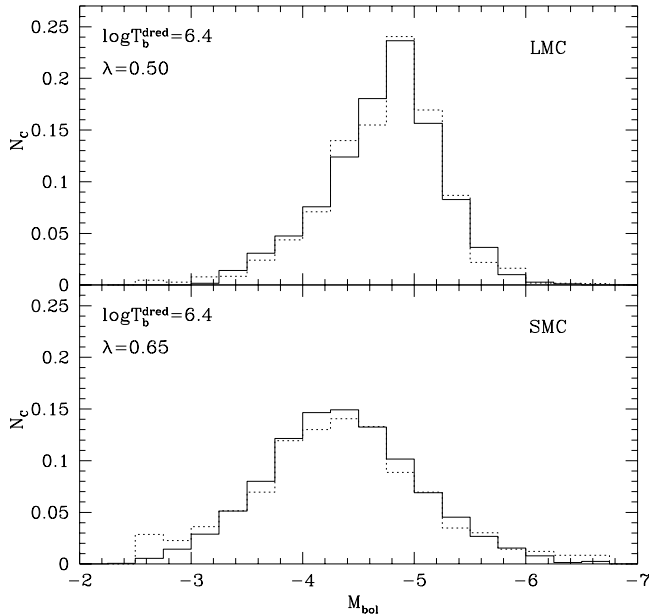


**Fig. 15.** Observed CSLFs (dotted line) in the LMC (top panel) and SMC (bottom panel), and the theoretical best fits (solid line).

(corresponding to C stars with  $M_i \sim 1.25 M_\odot$ ) to find abundances reduced by a factor of 2. Therefore, it is possible that  $Z = 0.002$  evolutionary tracks would be more suitable to represent the oldest (and faintest) SMC carbon stars. We remark, however, that the present investigation is intended to give a first hint about the behaviour of the dredge-up parameters at metallicities lower than  $Z = 0.008$ . Relevant transition luminosities as a function of the initial mass are displayed in Fig. 7, for two choices of the dredge-up parameters.

The best fit is obtained adopting ( $\log T_b^{\text{dred}} = 6.4$ ,  $\lambda = 0.65$ ) in the simple case of a constant SFR and Salpeter’s IMF as shown in the bottom panel of Fig. 15. It is interesting to notice that the proper value of  $T_b^{\text{dred}}$  is the same as for the LMC. This is in agreement with the indications from complete evolutionary calculations already discussed in Sect. 3.2, that  $T_b^{\text{dred}}$  is constant regardless of core mass and metallicity.

Another aspect worthy of notice is that a greater efficiency of the third dredge-up is required, if compared to the results for the LMC. This also agrees qualitatively with the indications from complete modelling of thermal pulses (e.g. Boothroyd & Sackmann 1988d) that a deeper envelope penetration is favoured at lower metallicities. As already mentioned, the effect of increasing  $\lambda$  is that of shifting the peak location towards fainter luminosities. Indeed, this is one of the most evident differences between the distributions of carbon stars in the two Clouds.

Concerning the broader extension in luminosity of the CSLF in the SMC if compared to the LMC, the following effects are remarked:

- The faint end of the distribution is reached at lower luminosities in the case of lower metallicities mainly because of both an earlier onset of the third dredge-up, and the smaller number of dredge-up episodes required for the transition to the C-class (due to the lower original abundance of oxygen in the envelope).
- As far as the bright end of the distribution is concerned, it is worth noticing that a good fit to the observed data for the SMC is obtained assuming a constant SFR over the entire significant age interval, without the recent drop (at an age of  $\sim 5 \times 10^8$  yr) invoked for the LMC.

The CSLFs for both Magellanic Clouds are presented in the two panels of Fig. 15. It is remarkable that the present formulation for the third dredge-up allows a good fitting of the CSLFs of both Clouds without any dramatic change in the input parameters. In this context, *the large difference between the CSLFs in the LMC and SMC are interpreted mainly as the result of a different metallicity*. The different histories of SFR in both galaxies probably play only a minor role in their CSLFs.

## 8. Conclusions

In this paper we describe an improved treatment of dredge-up in synthetic TP-AGB models, based on the adoption of the parameter  $T_b^{\text{dred}}$ , i.e. the minimum base temperature required for dredge-up to occur. Every time a thermal pulse is expected during calculations, envelope integrations are performed to check whether the condition on the base temperature is satisfied. It follows that, contrary to the test based on the constant  $M_c^{\text{min}}$  parameter, with this new scheme the response depends not only on the core mass but also on the current physical conditions of the envelope (i.e. the surface luminosity peak, the effective temperature, the mass, the chemical composition). Moreover, this method allows one to determine not only the onset, but also the possible shut-down of dredge-up occurring when the envelope mass is significantly reduced by stellar winds, without invoking further a priori assumptions.

This aspect is crucial. In fact, after the shut-down of the third dredge-up, surface and wind abundances of low-mass AGB stars are expected to freeze out till the end of the evolution, with important consequences for the chemical composition of planetary nebulae, which are ejected during the last evolutionary stages. Another point concerns the competition between envelope burning and dredge-up in the most massive TP-AGB stars. In particular, if the shut-down of dredge-up occurs after envelope burning extinguishes, a star might undergo a late conversion to carbon star. The recent detection of a luminous

( $M_{\text{bol}} \sim -6.8$ ) dust-enshrouded carbon star in the LMC (van Loon et al. 1998) seems to indicate such eventuality. This topic is the subject of a future study.

The CSLFs in the Magellanic Clouds are investigated as possible calibrators of the dredge-up parameters, and possible indicators of the SFR history in the host galaxies. We briefly summarise here the basic points emerging from our analysis:

- In principle, the observed CSLFs can provide indications on the SFR history within the age interval from about  $4 \times 10^9$  yr to  $\sim 10^8$  yr. Nothing can be inferred for younger ages.
- The faint end of the luminosity distribution is essentially determined by the temperature parameter  $T_{\text{b}}^{\text{dred}}$ .
- The peak location depends only weakly on the SFR, and hence it is a stringent calibrator of the efficiency parameter  $\lambda$ .
- Although the peak location is essentially invariant with respect to the SFR, the shape of the carbon star distribution may give hints on the history of the SFR in recent epochs (for ages between  $7 \times 10^8$  and  $10^8$  yr ago). However, the bright wing is expected to be sensitive to the details of physical processes occurring in the most massive stars, i.e. envelope burning and mass loss.
- The best fit to the observed CSLF in the LMC is obtained with  $\lambda = 0.50$ ,  $T_{\text{b}}^{\text{dred}} = 6.4$ , and a constant SFR up to an age of about  $5 \times 10^8$  yr. This recent drop of the SFR is invoked to remove a slight excess of bright carbon stars otherwise predicted.
- The best fit to the observed CSLF in the SMC is derived with  $\lambda = 0.65$ ,  $T_{\text{b}}^{\text{dred}} = 6.4$ , and a constant SFR over the entire significant age interval.
- If compared with the calibration for the LMC, a greater efficiency of dredge-up is required to reproduce the fainter peak of the CSLF in the SMC.

*Acknowledgements.* We are grateful to Cesare Chiosi for his important advice and kind interest in this work. We thank Achim Weiss for carefully reading the manuscript and for his useful comments. Peter Wood is acknowledged for the important suggestions which gave origin to the treatment of dredge-up here proposed. Many thanks to our referee, Arnold I. Boothroyd, whose remarks helped us to significantly improve the final version of this paper. The work by L. Girardi is funded by the Alexander von Humboldt-Stiftung. A. Bressan acknowledges the support by the European Community under TMR grant ERBFMRX-CT96-0086.

## References

- Alexander D.R., Ferguson J.W., 1994, ApJ 437, 879  
 Bertelli G., Mateo M., Chiosi C., Bressan A., 1992, ApJ 388, 400  
 Blanco V.M., McCarthy M.F., 1983, AJ 88, 1442  
 Blanco V.M., McCarthy M.F., Blanco B.M., 1980, ApJ 242, 938  
 Boothroyd A.I., Sackmann I.-J., 1988a, ApJ 328, 632  
 Boothroyd A.I., Sackmann I.-J., 1988b, ApJ 328, 641  
 Boothroyd A.I., Sackmann I.-J., 1988c, ApJ 328, 653  
 Boothroyd A.I., Sackmann I.-J., 1988d, ApJ 328, 671  
 Chandrasekhar S., 1939, An Introduction to the Study of Stellar Structure, The University of Chicago Press, Chicago  
 Chiosi C., Bertelli G., Bressan A., 1992, ARA&A 30, 235  
 Cohen J.G., Persson S.E., Elias J.H., Frogel J.A., 1981, ApJ 249, 481  
 Costa E., Frogel J.A., 1996, AJ 112, 2607  
 Da Costa G.S., Hatdizimitriou D., 1998, AJ 115, 1934  
 de Freitas Pacheco J.A., Barbuy B., Idiart T., 1998, A&A 332, 19  
 de Kool M., Green P.J., 1995, ApJ 449, 236  
 Dopita M.A., Vassiliadis E., Wood P.R., et al., 1997, ApJ 474, 188  
 Eggleton P.P., 1967, MNRAS 135, 243  
 Elson R., Fall, 1985, ApJ 299, 211  
 Ferrini F., Penco U., Palla F., 1990, A&A 231, 391  
 Forestini M., Charbonnel C., 1997, A&AS 123, 241  
 Frantsman J., 1997, A&A 319, 511  
 Freytag B., Ludwig H.G., Steffen M., 1996, A&A 313, 497  
 Frogel J.A., Mould J., Blanco V.M., 1990, ApJ 352, 96  
 Frost C.A., Lattanzio J.C., 1996, ApJ 473, 383  
 Frost C.A., Cannon R.C., Lattanzio J.C., Wood P.R., Forestini M., 1998, A&A 332, L17  
 Gallino R., Busso M., Picchio G., Raiteri C.M., 1990, Nat 348, 298  
 Gingold R.A., 1974, ApJ 193, 177  
 Gingold R.A., 1975, ApJ 198, 425  
 Girardi L., Chiosi C., Bertelli G., Bressan A., 1995, A&A 298, 87  
 Girardi L., Bressan A., Chiosi C., 1996, in 32nd Liège Int. Astrop. Coll., Stellar Evolution: What Should Be Done, eds. A. Noels, et al. Université de Liège, p. 39  
 Groenewegen M.A.T., 1998, in: ISO's view on Stellar Evolution, Conference Proc., Noordwijkerhout, The Netherlands, eds. L.B.F.M. Waters, C. Waelkens, K.A. van der Hucht, P.A. Zaal, Kluwer Academic Publ., Dordrecht, p. 379  
 Groenewegen M.A.T., de Jong T., 1993, A&A 267, 410  
 Herwig F., Blöcker T., Schönberner D., El Eid M., 1997, A&A 324, L81  
 Iben I., 1981, ApJ 246, 278  
 Iben I., Renzini A., 1982, ApJ 263, L23  
 Iben I., Renzini A., 1983, ARA&A 21, 27  
 Iben I., Renzini A., 1984, Phys. Rep. 105, 329  
 Iglesias C.A., Rogers F.J., 1996, ApJ 464, 943  
 Ivezić Z., Elitzur M., 1995, ApJ 445, 415  
 Kippenhahn R., 1981, A&A 102, 293  
 Koester D., 1987, ApJ 322, 852  
 Koester D., Reimers D., 1996, A&A 313, 810  
 Lattanzio J.C., 1986, ApJ 311, 708  
 Lattanzio J.C., 1987, ApJ 313, L15  
 Lattanzio J.C., 1989, ApJ 344, L25  
 Lattanzio J.C., Boothroyd A.I., 1997, in Astrophysical Implications of the Laboratory Study of Presolar Materials, AIP Conference Proc. 402, eds. Bernatowitz T., Zimmer E., AIP: Woodbury, NY, p. 85  
 Madore B.F., Freedman W.L., 1998, ApJ 492, 110  
 Marigo P., 1998a, PhD Thesis, University of Padova  
 Marigo P., 1998b, A&A 340, 463

- Marigo P., Bressan A., Chiosi C., 1996a, *A&A* 313, 545  
Marigo P., Girardi L., Chiosi C., 1996b, *A&A* 316, L1  
Marigo P., Bressan A., Chiosi C., 1998, *A&A* 331, 564  
Miller G.E., Scalo J.M., 1979, *ApJS* 41, 513  
Olszewski E.W., Schommer R.A., Suntzeff N.B., Harris H.C., 1991, *AJ* 101, 515  
Oudmaijer R.D., Groenewegen M.A.T., Schrijver H., 1998 *MNRAS* 294, L41  
Paczyński B., 1970, *Acta Astr.* 20, 195  
Panagia N., 1998, in *New Views of the Magellanic Clouds*, IAU Symp. 190, in press  
Rebeiro E., Azzopardi M., Westerlund B.E., 1993, *A&AS* 97, 603  
Refsdal S., Weigert A., 1970, *A&A* 6, 426  
Richer H.B., Olander N., Westerlund B.E., 1979, *ApJ* 230, 724  
Russell S.C., Dopita M.A., 1990, *ApJS* 74, 93  
Salaris M., Cassisi S., 1998, *MNRAS* 298, 166  
Salpeter E.E., 1955, *ApJ* 121, 161  
Schmidt H., 1995, *Diplom Thesis*, Universität Kiel  
Schwarzschild M., 1958, *Structure and Evolution of the Stars*, University Press, Princeton  
Schönberner D., 1979, *A&A* 79, 108  
Straniero O., Chieffi A., Limongi M., et al., 1997, *ApJ* 478, 332  
Tinsley B.M., 1980, *Fundam. of Cosmic Phys.* 5, 287  
Tuchman Y., Glasner A., Barkat Z., 1983, *ApJ* 268, 356  
van Loon J.Th., Zijlstra A.A., Whitelock P.A., et al., 1998, *A&A* 329, 169  
Vassiliadis E., Wood P.R., 1993, *ApJ* 413, 641  
Wagenhuber J., 1996, *PhD thesis*, TU München  
Wagenhuber J., Groenewegen M.A.T., 1998, *A&A* 340, 183  
Westerlund B.E., 1990, *A&AR* 2, 29  
Westerlund B.E., Olander N.O., Richer H.B., Crabtree D.R., 1978, *A&AS* 31, 61  
Westerlund B.E., Azzopardi M., Breysacher J., 1986, *A&AS* 65, 79  
Westerlund B.E., Azzopardi M., Rebeiro E., Breysacher J., 1991, *A&AS* 91, 425  
Westerlund B.E., Azzopardi M., Breysacher J., Rebeiro E., 1995, *A&A* 303, 107  
Wood P.R., 1981, in: *Physical processes in red giants*, Proc. of the Second Workshop, Erice, Italy (September 3-13, 1980), Dordrecht, D. Reidel Publishing Co., p. 135  
Wood P.R., Zarro D.M., 1981, *ApJ* 247, 247  
Wood P.R., Arnold A., Sebo K.M., 1997, *ApJL* 485, L25